# Event-by-event investigation of the two-particle source function in heavy-ion collisions with EPOS

22nd ZIMÁNYI SCHOOL
WINTER WORKSHOP
ON HEAVY ION PHYSICS

December 5-9, 2022
Budapest, Hungary

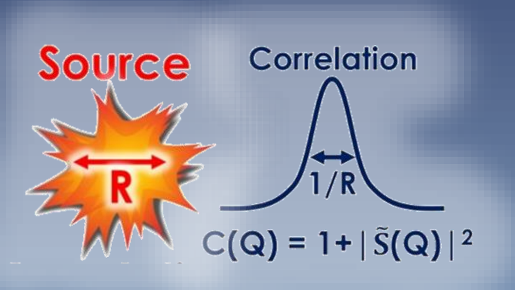


- Experiments: measuring C(Q) mom. corr. to gain information about D(r) pair source
- Event generators: D(r) directly available!
- Experimental indications – power-law component in pion pair-source – Lévy shape?

$$C(Q,K) = \frac{\int D(r,K)\left|\psi_Q(\mathrm{r})\right|^2 dr}{\int D(r,K)dr}$$

- $Q$: relative pair momentum
- $K$: average pair momentum
- $r$: relative coordinate
- $\psi_Q$: Pair wave func., contains FSI

$$\mathcal{L}(\alpha,R;r) = \frac{1}{(2\pi)^3}\int d^3q e^{iqr} e^{-\frac{1}{2}|qR|^\alpha}$$

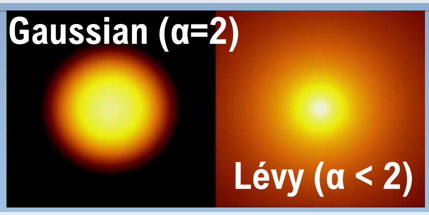



**DÁNIEL KINCSES**, EÖTVÖS UNIVERSITY, BUDAPEST

IN COLLABORATION WITH BALÁZS KÓRODI, MÁTÉ CSANÁD

ELTE EÖTVÖS LORÁND UNIVERSITY

Csörgő, Hegyi, Zajc, Eur.Phys.J. C36 (2004) 67-78; Csanád, Csörgő, Nagy, Braz.J.Phys. 37 (2007) 1002;
Csörgő, Hegyi, Novák, Zajc, AIP Conf.Proc. 828; Csörgő, Hegyi, Novák, Zajc, Acta Phys.Polon. B36
Metzler, Klafter, Physics Reports 339 (2000) 1-77; Kincses, Stefaniak, Csanád, Entropy 24 (2022) 3, 308

# Appearance of Lévy-type sources in heavy-ion collisions (Au+Au @ 200 GeV)

- **Possible (competing) reasons for the appearance of Lévy-type sources:**
  1. (Jet fragmentation)
  2. (Proximity of the critical endpoint)
  3. **Event averaging (different shapes)?**
  4. **Resonance decays?**
  5. **Anomalous diffusion?**
- **EPOS 200 GeV Au+Au collisions: Event-by-event non-Gaussianity!!!**
  - Single-event Lévy fits → good description
  - power-law tail strongly affected by rescattering, decays; $2 > \alpha_{EPOS} > \alpha_{exp}$
  - Lévy shape not from event averaging!

*D. Kincses, M. Stefaniak, M. Csanád, Entropy 24 (2022) 3, 308*

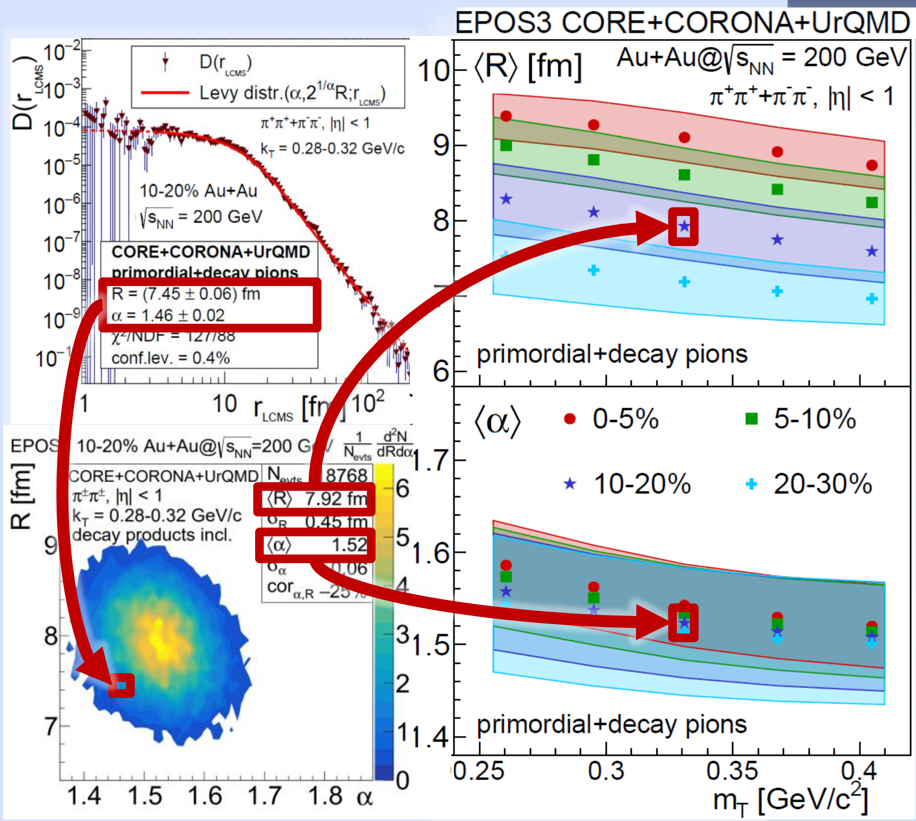

# Appearance of Lévy-type sources in heavy-ion collisions (Pb+Pb @ 2.76 TeV)

- **Brand new results for EPOS Pb+Pb @ 2.76 TeV**
  arXiv:2212.02980

- $m_T$ dependence of Lévy source parameters
- Effect of resonance decays
- Particle species dependence
- New scaling behavior observed

- **Check out the poster for more details!**

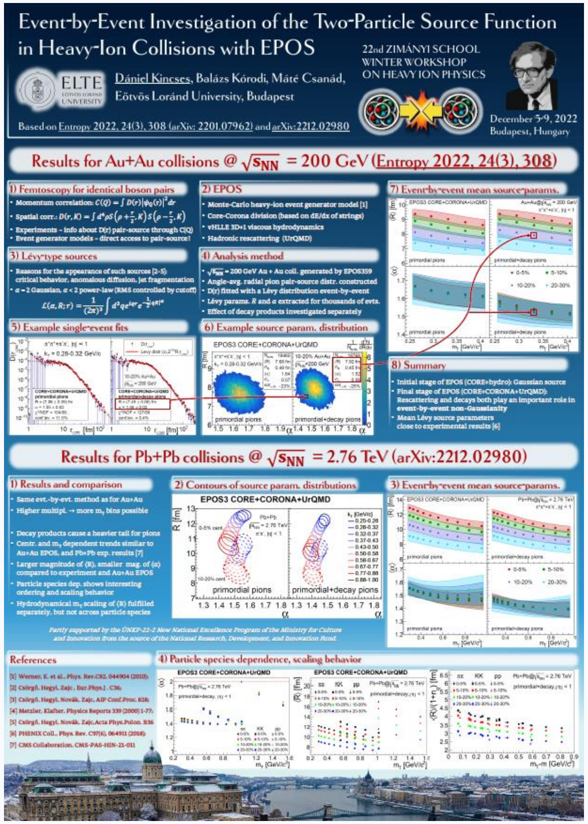

# Femtoscopic correlation of kaons

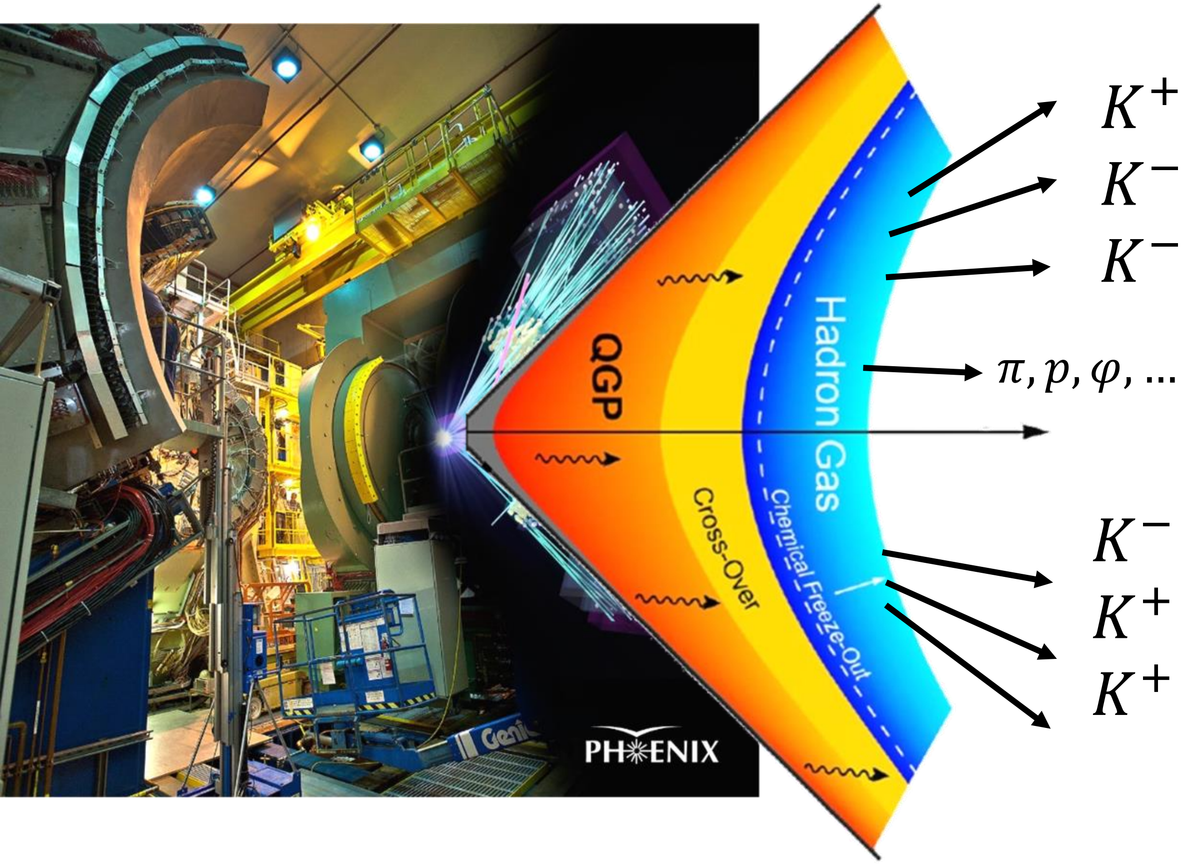


Hanbury-Brown and Twiss: intensity correlation

Goldhaber et al. in HEP

Access the spatio-temporal structure of the particle emitting source

$$C_2(p_1, p_2) = \frac{N_2(p_1, p_2)}{N_1(p_1) N_1(p_2)}$$

use Yano-Koonin formula to relate the momentum distribution to the emitting source

$$\underbrace{N_2(p_1, p_2)}_{\text{Two-particle momentum distr.}} = \int \underbrace{dx_1 dx_2}_{\text{Space-time coordinates}} \underbrace{S(x_1, p_1) S(x_2, p_2)}_{\text{Source functions}} \underbrace{|\Psi_2(x_1, x_2)|^2}_{\text{Two-particle wavefunction}}$$

Two-particle momentum distr.

Space-time coordinates

Source functions
What shape?

Two-particle wavefunction
FSI here, i.e., Coulomb, strong

# On the shape of the correlation function

Generalized Gaussian – Levy distribution

$$\mathcal{L}(\alpha,R,r)=\frac{1}{(2\pi)^3}\int d^3q\, e^{iqr}e^{-\frac{1}{2}|qR|^{\alpha}}$$

$\alpha=2$: Gaussian, $\alpha=1$: Cauchy, $0<\alpha\leq 2$: Levy

Rel. mom. in LCMS
1D variable!

Assume the source to be Levy! $\Rightarrow$ Correlation: $C_2(Q)=1+\lambda e^{(RQ)^{\alpha}}$

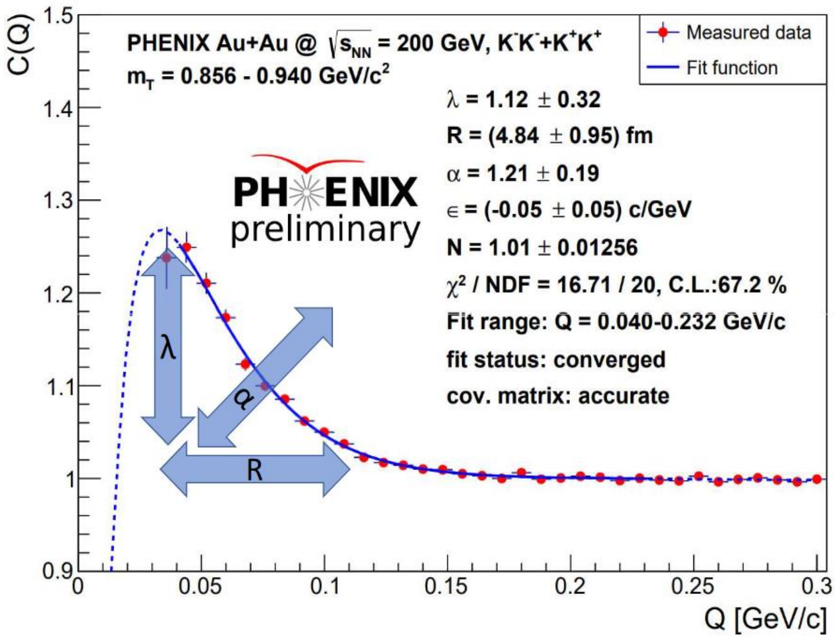


Distortion effects:
Coulomb, strong FSI to be included!
Resonances, coherence, …

$\lambda(K)$: core-halo parameter
$R(\mathrm{K})$: Levy-scale parameter
$\alpha(K)$: Levy index of stability

# Experimental results from PHENIX

- $\pi$: 0-30% centrality selection
- K: minimum bias, still comparable
- Levy-index agree for $\pi$ and $K$ $\Rightarrow$ common Levy-process?
- Core-halo parameter: $\pi$ and $K$ compatible
- Levy-scale parameter: hydro scaling,
- $\pi$ and $K$ compatible, despite $R_{Levy} \neq R_{Gauss}$

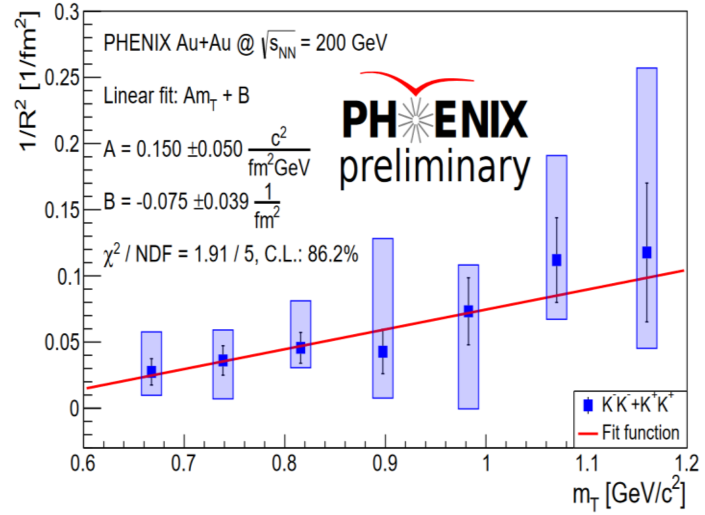


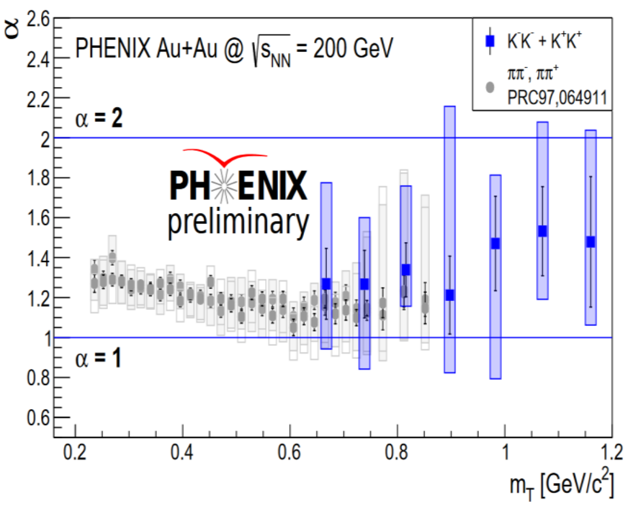


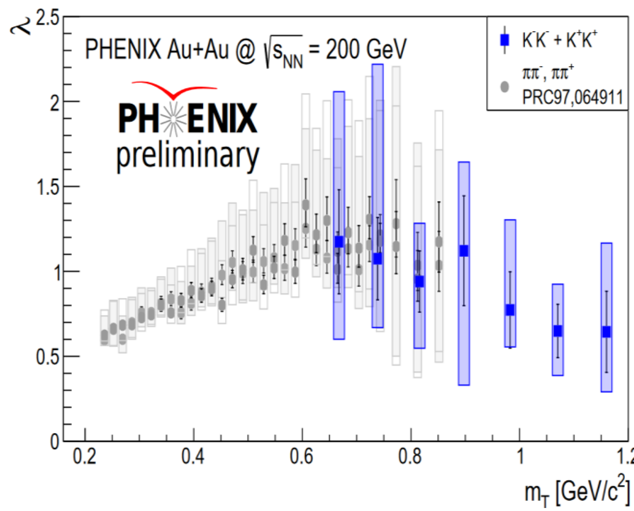


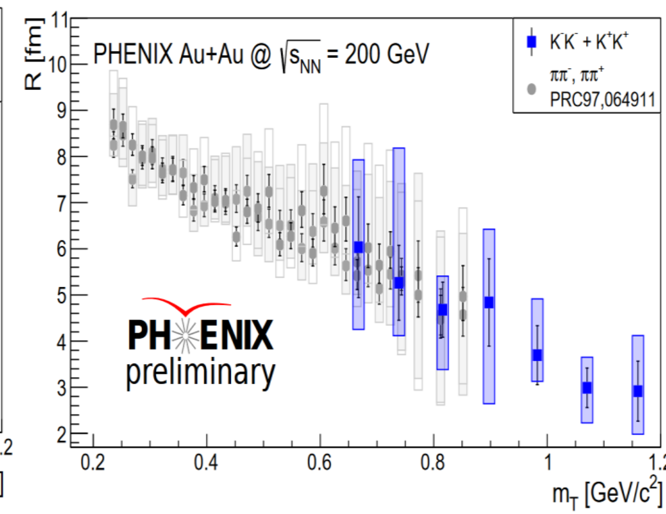

[1] Acta Phys. Polon. B36 (2005) 329-337
[2] AIP Conf. Proc. 828 (2006) no.1, 525-532
[3] Braz. J. Phys. 37 (2007) 1002

# Lévy HBT

- Momentum correlation ↔ source function : $C(q) \approx 1 + \left|\tilde{S}(q)\right|^2$
- Lévy distribution: $L(\boldsymbol{r}; \alpha, R) = (2\pi)^{-3} \int d^3\boldsymbol{q} e^{i\boldsymbol{qr}} e^{-\frac{1}{2}|\boldsymbol{q}R|^{\alpha}}$
- Many possible reasons[1,2,3] i.e. anomalous diffusion, critical phenomena …
- Lévy-type source + core-halo model: $C(q) = 1 + \lambda e^{-|qR|^{\alpha}}$
- Detailed centrality-dependent Lévy shape analysis
  - Measurement of:
    - ➢ Lévy stability index $\alpha$ → shape
    - ➢ Lévy scale parameter $R$ → spatial scale
    - ➢ Correlation strength $\lambda$ → core-halo, partial coherence
  - Study the centrality and $m_T$ dependence

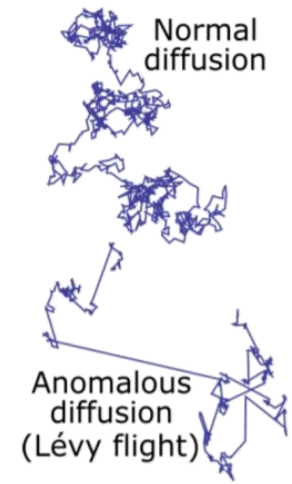


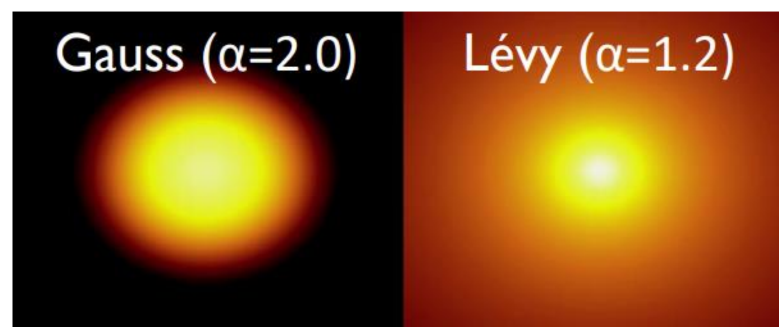

[1]*Phys. Lett. B 432, (1998) 248*
[2]*Phys. Part. Nucl. 51, (2020) 238*

# Analysis details

- 5.02 TeV PbPb data from CMS
- Calculate the correlation function:

$$C(q) = \frac{A(q)}{B(q)} \cdot \frac{\int B}{\int A}$$

  - A(q) actual (same event) pair distribution
  - B(q) background (mixed event) pair distribution
- Remove long-range background→ DR(q)
- Obtain the parameters via fitting[1,2]:

$$DR(q) = N(1+\varepsilon q)\left[1-\lambda+\lambda\left(1+e^{-|qR|^{\alpha}}\right)K_C(q;\alpha,R)\right]$$

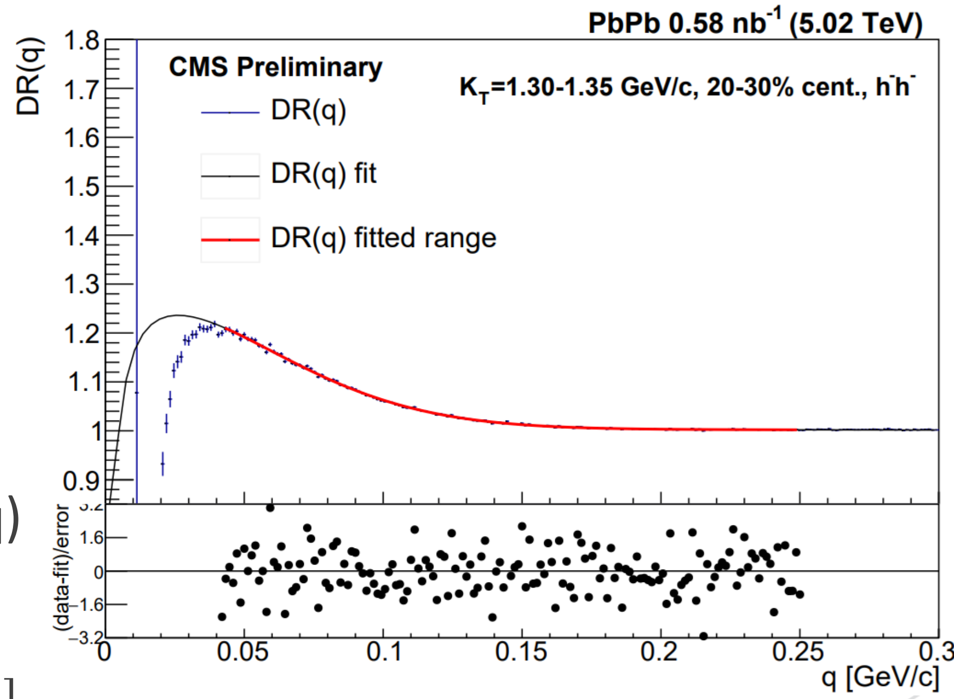

# Main results

- Lévy source shape
- $\alpha$ between 1.6 and 2.0
  - Centrality-dependent
  - Constant in $m_T$
- Hydro-like linear scaling: $^1/_{R^2} \sim m_T$
- $R$ linear scaling in $\left\langle N_{\text{part}}^{1/3} \right\rangle \longrightarrow$ spatial scale
- Decreasing λ vs. $m_T$
  - Caused by the lack of particle id.
- For details see the upcoming poster or [CMS-PAS-HIN-21-011](CMS-PAS-HIN-21-011)

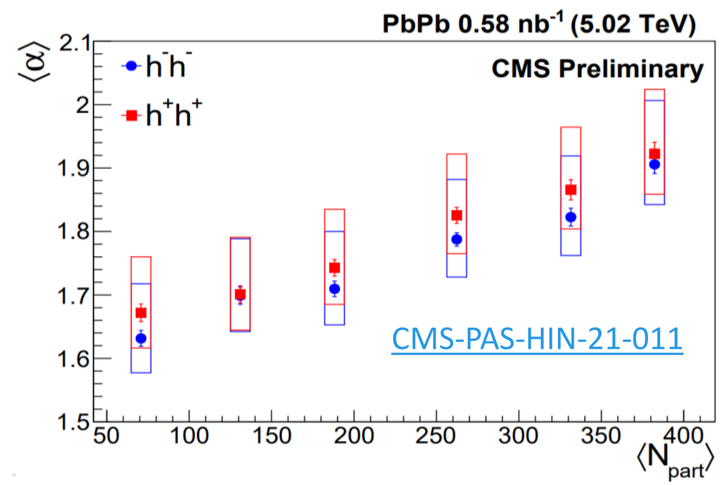


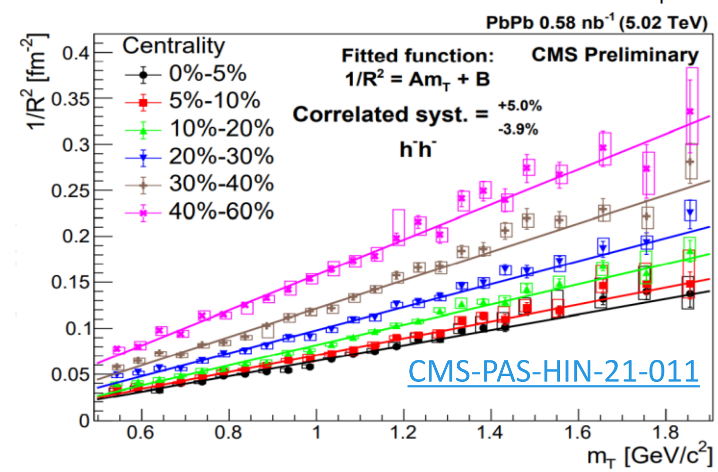


*Supported by the ÚNKP-21-2 New National Excellence Program of the Ministry for Innovation and Technology from the source of the National Research, Development and Innovation Fund.*

22nd Zimanyi School
Winter Workshop on Heavy Ion Physics

AGH
AGH University of Science and Technology

# Cumulants with global baryon conservation and short-range correlations

Michał Barej

AGH University of Science and Technology, Kraków, Poland

In collaboration with Adam Bzdak

Supported by NCN, Grant 2018/30/Q/ST2/00101

barej@agh.edu.pl

# The conjectured QCD phase diagram

- Most of this is only an educated guess based on effective models.
- Search for the critical point - conserved charges fluctuations (cumulants, factorial cumulants).
- Experiments: heavy-ion collisions at different energies.
- Background:
  - small fluctuations of the impact parameter
  - **global baryon number conservation**

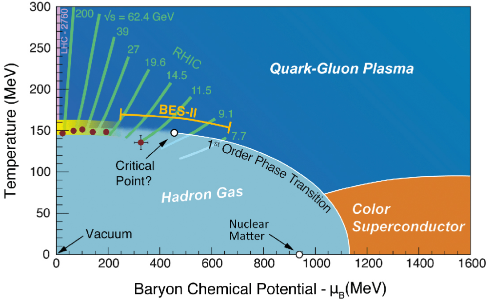


A. Bzdak, S. Esumi, V. Koch, J. Liao, M. Stephanov and N. Xu, Phys. Rept. **853**, 1-87 (2020)
A. Aprahamian, A. Robert, H. Caines, *et al.*, *Reaching for the horizon: The 2015 long range plan for nuclear science*

# Cumulants with baryon conservation and short-range correlations obtained from the cumulants without baryon conservation.

$$\kappa_n^{(1,B)} \approx \underbrace{\kappa_n^{(1,B,\mathrm{LO})}}_{\substack{\propto B^1 \\ \text{thermodynamic limit}}} + \underbrace{\kappa_n^{(1,B,\mathrm{NLO})}}_{\propto B^0} + \underbrace{\ldots}_{O(B^{-1})}$$

$$\kappa_1^{(1,B)} = fB = f\kappa_1^{(G)}$$

$$\kappa_2^{(1,B,\mathrm{LO})} = \bar{f} f \kappa_2^{(G)}$$

$$\kappa_2^{(1,B,\mathrm{NLO})} = \frac{1}{2}\bar{f} f \frac{(\kappa_3^{(G)})^2 - \kappa_2^{(G)}\kappa_4^{(G)}}{(\kappa_2^{(G)})^2}$$

$$\kappa_3^{(1,B,\mathrm{LO})} = \bar{f} f (1-2f)\kappa_3^{(G)}$$

$$\kappa_3^{(1,B,\mathrm{NLO})} = \frac{1}{2} f\bar{f}(1-2f)\frac{\kappa_3^{(G)}\kappa_4^{(G)} - \kappa_2^{(G)}\kappa_5^{(G)}}{(\kappa_2^{(G)})^2}$$

$$\kappa_4^{(1,B,\mathrm{LO})} = f\bar{f}\left[\kappa_4^{(G)} - 3f\bar{f}\left(\kappa_4^{(G)} + (\kappa_3^{(G)})^2/\kappa_2^{(G)}\right)\right]$$

$$\kappa_4^{(1,B,\mathrm{NLO})} = \frac{1}{2} f\bar{f}\left\{\frac{\kappa_3^{(G)}\kappa_5^{(G)} - \kappa_2^{(G)}\kappa_6^{(G)}}{(\kappa_2^{(G)})^2} + 3f\bar{f}\left[\frac{(\kappa_4^{(G)})^2 + \kappa_2^{(G)}\kappa_6^{(G)}}{(\kappa_2^{(G)})^2} + \frac{2(\kappa_3^{(G)})^4 - 5\kappa_2^{(G)}(\kappa_3^{(G)})^2\kappa_4^{(G)} + (\kappa_2^{(G)})^2\kappa_3^{(G)}\kappa_5^{(G)}}{(\kappa_2^{(G)})^4}\right]\right\}$$

LO reproduces net-baryon cumulants from

V. Vovchenko, O. Savchuk, R.V. Poberezhnyuk, M.I. Gorenstein, V. Koch, PLB **811**, 135868 (2020)

NLO is new.

$\kappa_n^{(1,B)}$ - cumulants in the subsystem with the baryon conservation and short-range correlations

$\kappa_n^{(G)}$ - short-range cumulants in the whole system without baryon conservation

$f$ - a fraction of particles in the acceptance, $\bar{f} = 1 - f$

# Example

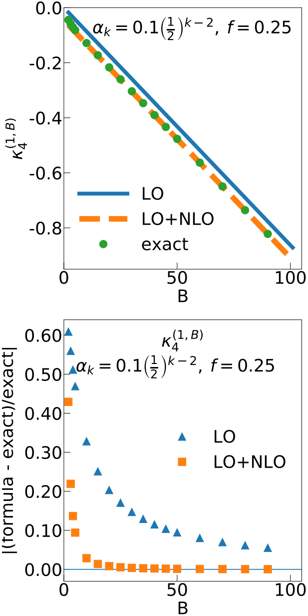


- exact - a straightforward differentiation of the factorial cumulant gen. func.,
- $\alpha_k$ - k-particle short-range correlation strength, $\alpha_k = 0.1\left(\frac{1}{2}\right)^{k-2}$, $k = 2...6$, $\alpha_1 = 1$,
- $f$ - a fraction of particles in the acceptance.

- NLO improves the results.

MB and A. Bzdak, PRC 106, no. 2, 024904 (2022)

MB and A. Bzdak, [arXiv:2210.15394 [hep-ph]]

# Event-shape-dependent analysis of charm-anticharm correlations in simulations


Anikó Horváth[1 2] together with Eszter Frajna[1], Róbert Vértesi[1]

Zimányi School Winter Workshop on Heavy Ion Physics, 2022.


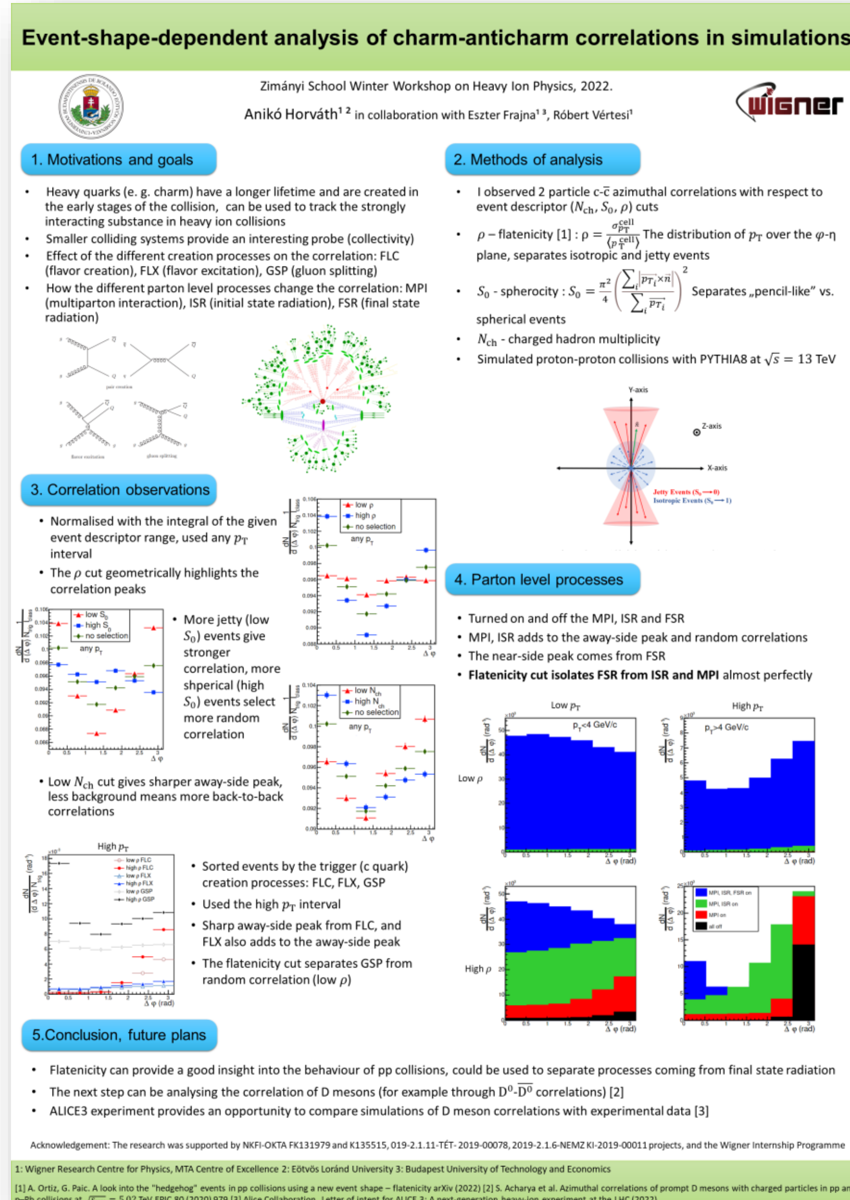



1 Wigner Research Centre for Physics, MTA Centre of Excellence
2 Eötvös Loránd University



The research was supported by NKFI-OKTA FK131979 and K135515 , and 019-2.1.11-TÉT- 2019-00078, 2019-2.1.6-NEMZ KI-2019-00011 projects, and the Wigner Intern Programme

# Motivation

- In heavy ion collisions, heavy quarks (charm) can be used to track the behaviour of the collision (long lifetime)
- Smaller collision systems provide an interesting probe (collectivity)
- Effects of parton level processes (multiparton interaction (MPI), initial (ISR) and final state radiation (FSR) )
- Effect of quark creation process on the correlation: flavor creation, flavor excitation, gluonsplitting

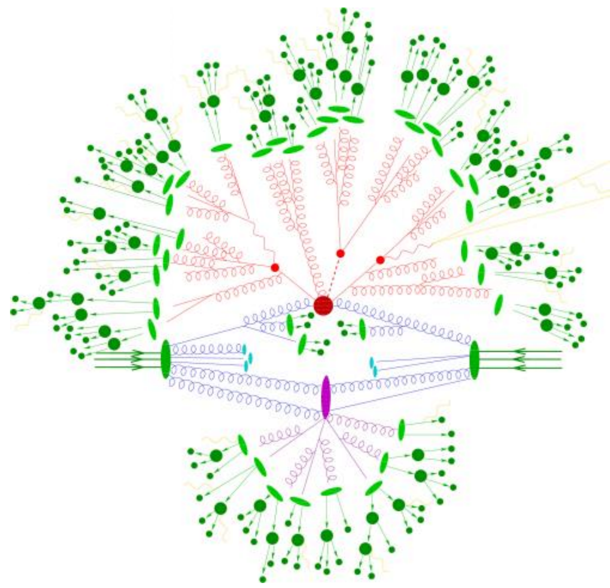

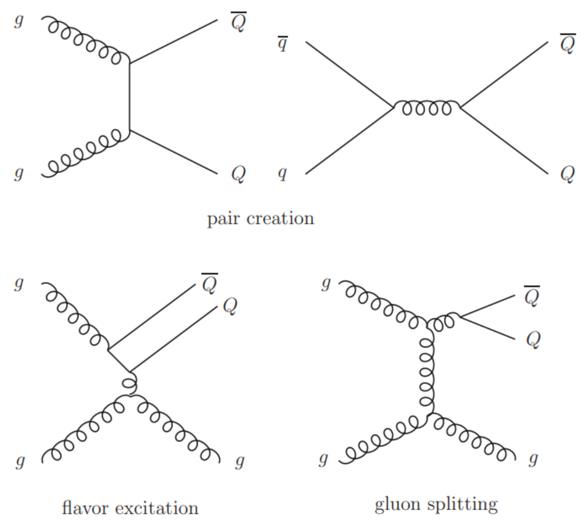

# Methods

- I used 2 particle c-$\bar{c}$ azimuthal correlations with respect to event descriptors ($N_{\mathrm{ch}}$, $S_0$, $\rho$)
- Flatenicity: the distribution of $p_{\mathrm{T}}$ in the $\varphi$-η plane
- $\rho$ highlights the correlation peaks
- Simulated pp (proton-proton) collisions with PYTHIA8 ($\sqrt{s} = 13$ TeV)

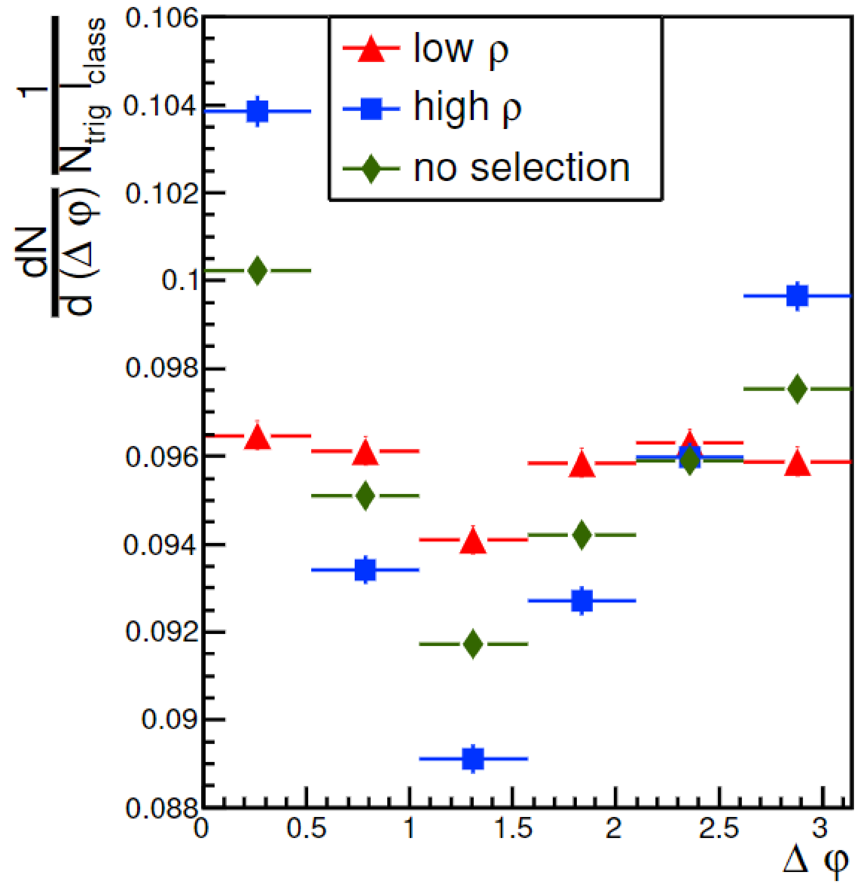


$$\rho = \frac{\sigma_{p_{\mathrm{T}}}^{\mathrm{cell}}}{\langle p_{\mathrm{T}}^{\mathrm{cell}} \rangle}$$

# Parton level processes

- Low: $p_{\mathrm{T}} < 4$ GeV/c,
  High: $p_{\mathrm{T}} > 4$ GeV/c
- Hard process, MPI, ISR: away-side peak, random correlations
- FSR: near-side peak

- **Flatenicity cut isolates FSR from ISR and MPI both at low and high $p_T$**

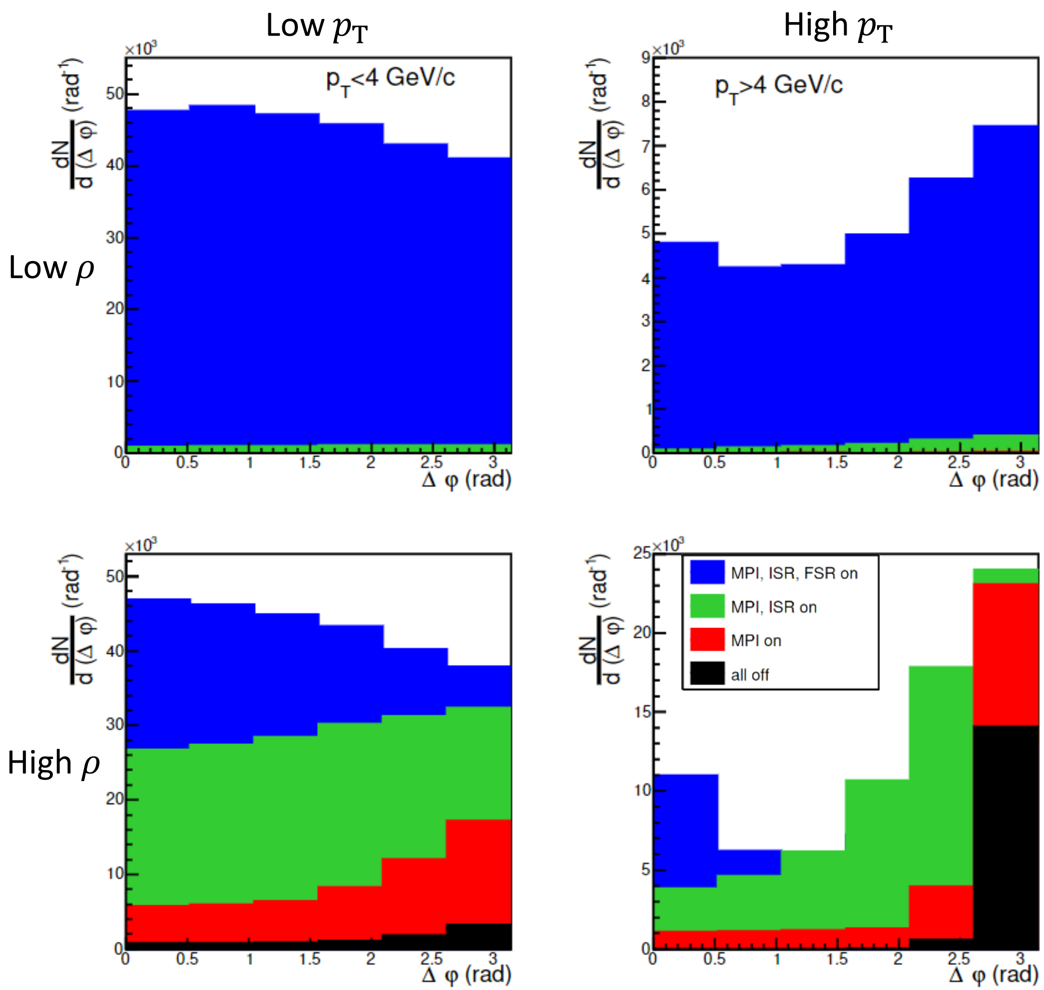

# Zimányi 2022
# Event activity dependence of charm baryon production at LHC energies

**Zoltán Varga**[1,2], **Róbert Vértesi**[1]

1. Wigner Research Centre for Physics

2. Budapest University of Technology and Economics

MŰEGYETEM 1782

# Production of heavy-flavor baryons

- Heavy-flavor production is usually described with the factorization approach: incoming **hadron PDFs**, hard **parton-parton scattering** and **fragmentation** are independent:

$$d\sigma^{hard}_{AB\to C} = \sum_{a,b} f_{a/A}(x_a, Q^2) \otimes f_{b/B}(x_b, Q^2) \otimes d\sigma^{hard}_{ab\to c}(x_a, x_b, Q^2) \otimes D_{c\to C}(z, Q^2)$$

Parton Distribution Function (PDF)

Partonic hard scattering cross-section

Fragmentation Function (FF)

- Traditional assumption: fragmentation functions are universal for different collision systems.
- Experimental results (ALICE, CMS, LHCb): significant enhancement in the $\Lambda_C/D^0$ ratio in the semi-soft $p_T$ range (2-8 GeV/c), compared to predictions from e+e-: **no universality**!
- **Color reconnection beyond leading color** (CR-BLC): Describes the multiplicity dependence.
- Multiplicity dependence: **connected to the event activity**! Needs to be better understood!

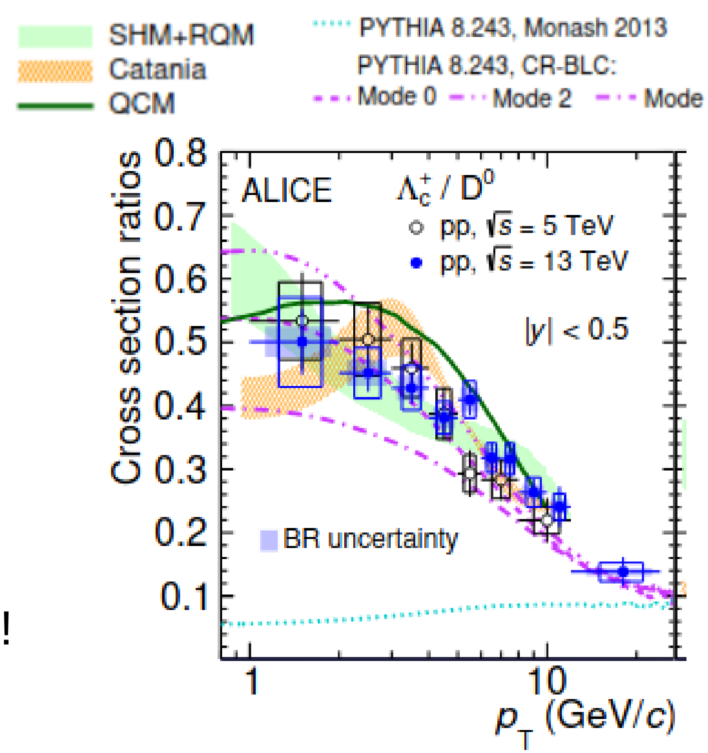

# $\Lambda_C/D^0$ enhancement classified by spherocity and flatenicity

**Z.V., R.V., J. Phys. G: Nucl. Part. Phys. 49 (2022) 075005 (arXiv:2111.00060)**

$\Lambda_c$(qqc), I = 0

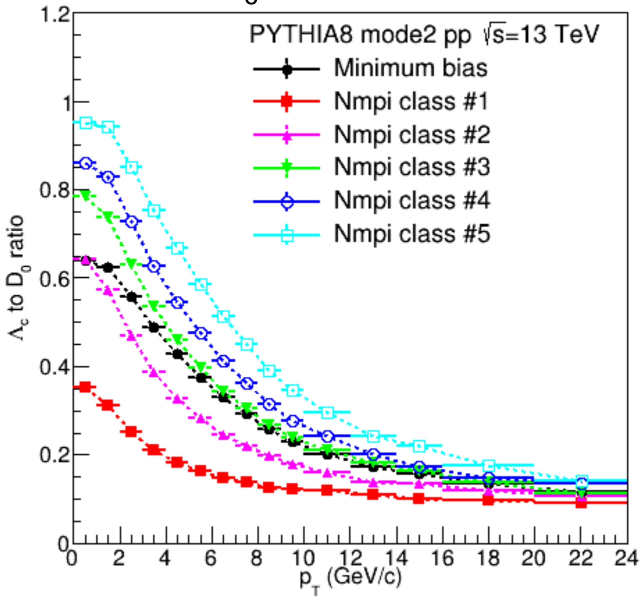


$$S_0 = \frac{\pi^2}{4} \times \min_{\hat{n}=(n_x,n_y,0)} \left( \frac{\Sigma_i |\vec{p}_{T_i} \times \hat{n}|}{\Sigma_i \vec{p}_{T_i}} \right)^2$$

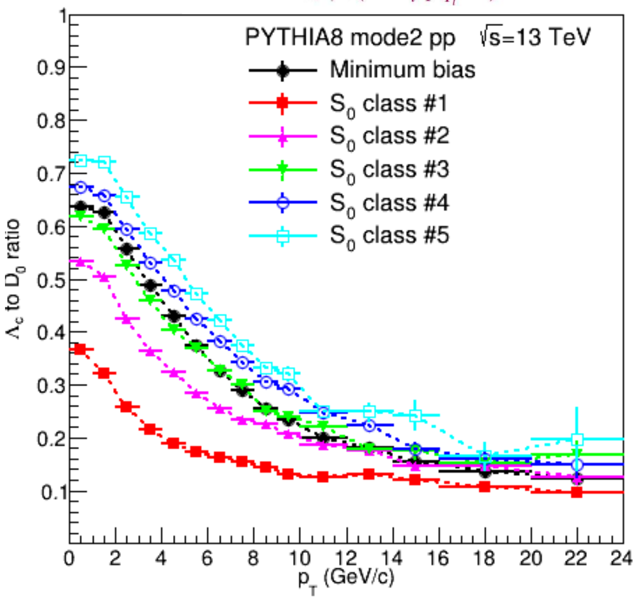


**<u>Flatenicity</u>: A. Ortiz, G. Paic, arXiv:2204.13733**

$$\rho = \sigma_{pT}^{cell} / \langle p_T^{cell} \rangle$$

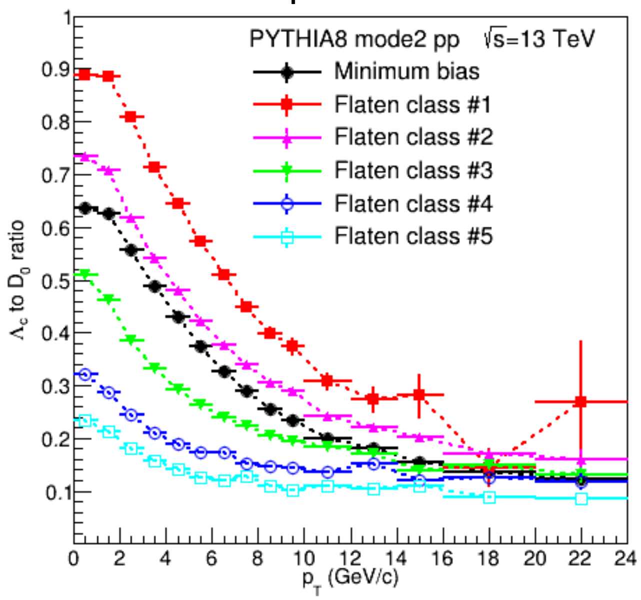


- The $\Lambda_C/D^0$ enhancement depends on the MPI in the lower $p_T$ region.
- Spherocity allows decribing the enhancement in events without a leading trigger hadron.
- **<u>Flatenicity</u> pulls apart the distributions much more than spherocity.**

# $\Lambda_C/D^0$ enhancement in jetty and isotropic events

Z.V., R.V., J. Phys. G: Nucl. Part. Phys. 49 (2022) 075005 (arXiv:2111.00060)

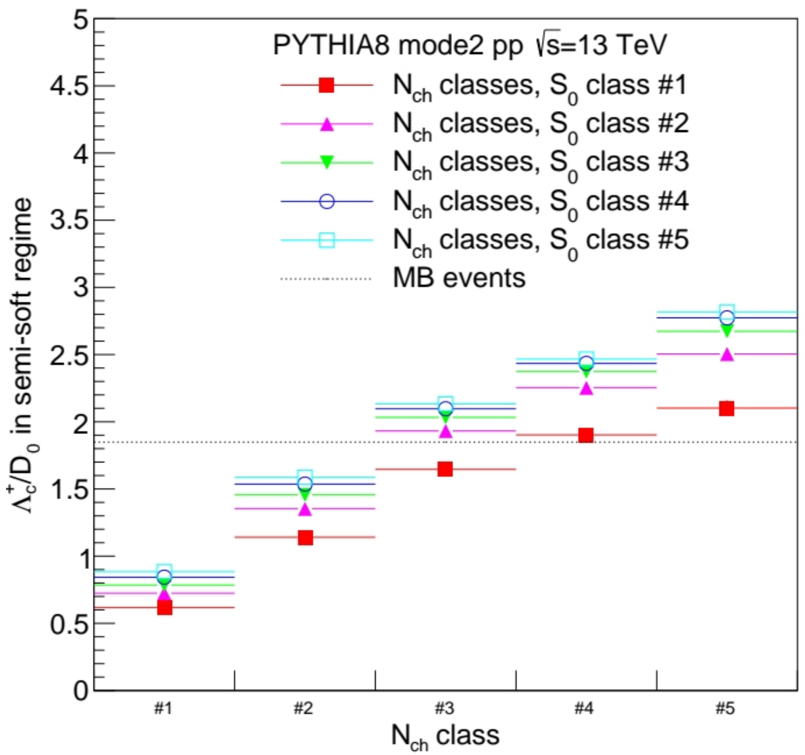


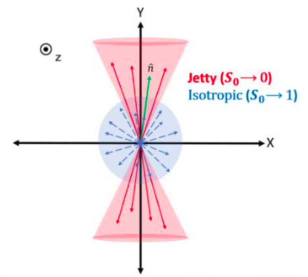


$$S_0 = \frac{\pi^2}{4} \times \min_{\hat{n}=(n_x,n_y,0)} \left( \frac{\Sigma_i |\vec{p}_{T_i} \times \hat{n}|}{\Sigma_i \vec{p}_{T_i}} \right)^2$$

$\rho = \sigma_{pT}^{cell} / \langle p_T^{cell} \rangle$

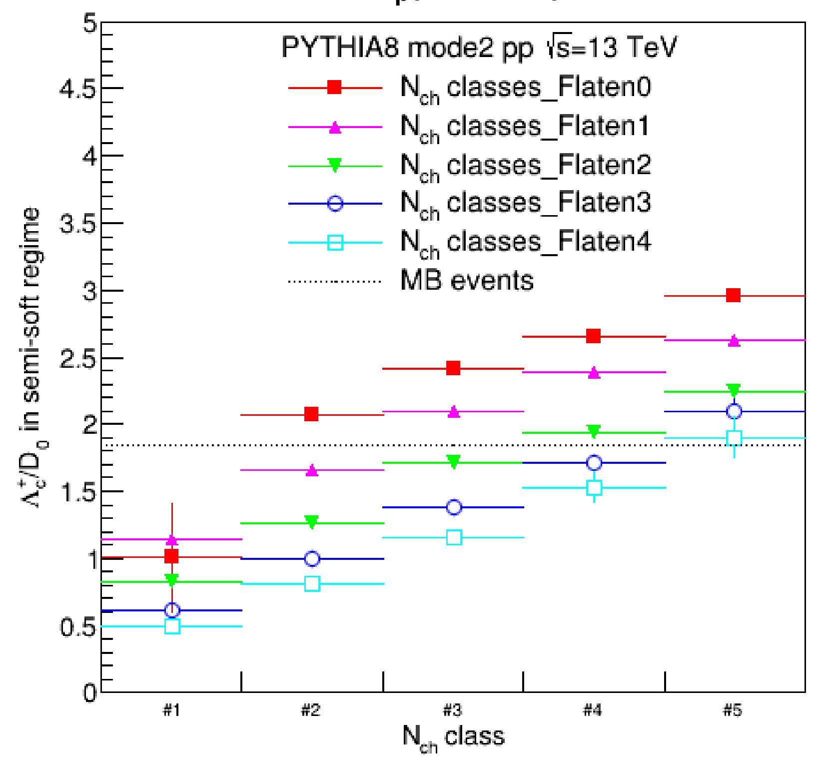


- **Spherocity $S_0$** in **minimum-bias events**:
  - $\Lambda_C/D^0$ enhancement is more prominent in spherical (UE-dominated) than jetty events
- **Flatenicity ρ** in **minimum-bias events**:
  - $\Lambda_C/D^0$ enhancement decreases with flatenicity, and **contrary to spherocity** the enhancement is sensitive to it in every $N_{ch}$ classes

- **CR-BLC model links the enhancement to the UE:**
  - discrimination power in data from the upcoming LHC Run3.
- **Flatenicity could be a better quantity to describe the MPI and the enhancement!**

# Analysis of $\pi^0$ in the large 2014 200 GeV Au+Au dataset

In 2014 large amount of Au+Au data were collected. This makes it possible to extend the transverse momentum range and improve the systematic uncertainties.

## Study DHM (dead-hot-map)

Applying several condition then organize these parameters in our analysis's "DHM" will help to identify the malfunctioning towers.

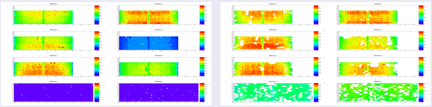

Figure: Raw hit map befor (the left side) & after (the right side) applying DHM.

## Apply DHM

As a result, here we apply the final DHM to see how does it work.

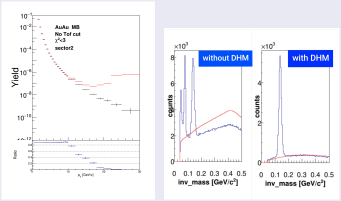


Figure: $\gamma$ (w/wo)-DHM (left) & The invariant mass distributions of $\pi^0$ (right).

## The Method of $\pi^0$ Extraction

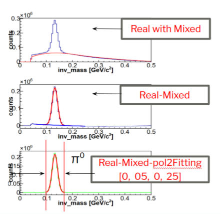


Figure: Mixed Event Background Subtraction Method (low $p_T$).

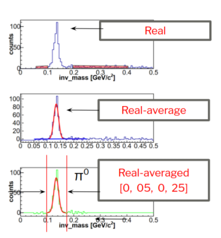


Figure: Background Subtraction by Average Bin Content (High $p_T$).

## Raw $\pi^0$ in centrality classes (MB)

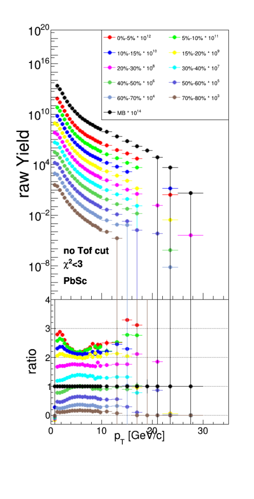


Figure: The raw yield of $\pi^0$ in centrality bins(upper) and the ratios of individual centrality to MB(lower).

## Raw $\pi^0$ from MB & ERT trigger

Comparison of the raw $\pi^0$ yields in different centrality bins indicates that the shapes at high $p_T$ vary only slowly, as found in earlier publications.

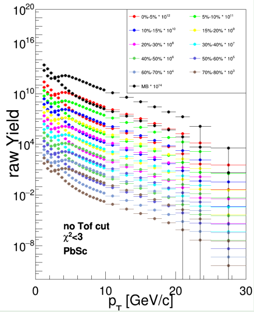


Figure: The raw yield of pi0 in centrality classes for MB & ERT trigger.

## Summary

- PHENIX measurement of $\pi^0$ & direct photons at high $p_T$ reachable at RHIC.
- This poster reports on the work in progress of the analysis of 2014, with statistics exceeding all previous data combined .
- The methods clarify the importance of data QA.
- Since these are uncorrected, raw data and the acceptance, efficiency and smearing corrections are large and strongly centrality dependent, no physics conclusions drawn yet.

# Probing flow fluctuation through factorization breaking in heavy-ion collision

- based on P. Bozek, R. Samanta, PRC 105, 034904 (2022)

**Rupam Samanta**

PhD Supervisor : Prof. dr. hab. Piotr Bożek

Faculty of Physics and Applied Computer Science
AGH University of Science and Technology, Krakow

NCN grant : 2019/35/O/ST2/00357

Dec 8, 2022

AGH University of Science and Technology
AGH


National Science Centre Poland

# Fluctuation of collective flow in HI Collisions

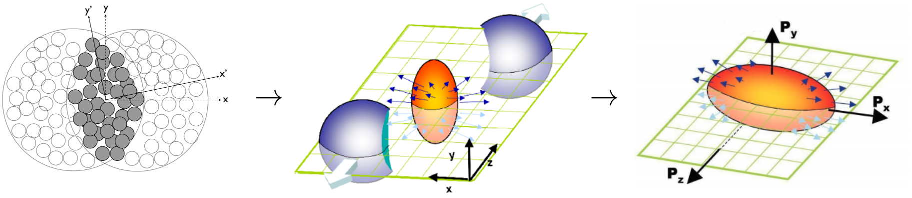


**Asymmetry in initial source distribution ⟶ Hydrodynamic evolution of the fireball ⟶ Final state momentum anisotropy**

## Momentum anisotropy : Harmonic flow

$$\frac{dN}{dp d\phi} = \frac{dN}{2\pi dp}\left(1 + 2\sum_{n=1}^{\infty} V_n(p) e^{in\phi}\right)$$

- Flow vector, $V_n = |V_n|\ e^{i\ n\Psi_n}$
  $|V_n| \rightarrow$ Flow magnitude & $\Psi_n \rightarrow$ Flow angle
- **Event by event fluctuation of initial state $\Longrightarrow$ event by event fluctuation of flow vectors $V_n$'s**

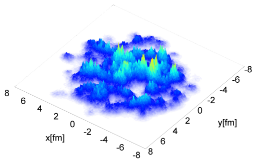


**lumpy structure of the initial density**

# Mapping flow fluctuation by factorization-breaking coefficients

- **Flow fluctuation** $\longrightarrow$ **decorrelation between two flow vectors in two momentum bins** $\longrightarrow$ **includes both flow magnitude and flow angle decorrelation** $\longrightarrow$ *factorization-breaking coefficients* .
- **Flow magnitude and flow angle decorrelation require 2nd order correlations** $\longrightarrow$ one flow momentum dependent $(V_n(p))$ and other flow momentum averaged $(V_n)$, removes experimental difficulty.
- The **flow vector square and flow magnitude square factorization coefficients** are constructed as,

$$r_{n;2}(p) = \frac{\langle V_n^2 V_n^*(p)^2 \rangle}{\sqrt{\langle |V_n|^4 \rangle \ \langle |V_n(p)|^4 \rangle}} \quad \text{and} \quad r_n^{v_n^2}(p) = \frac{\langle |V_n|^2 |V_n(p)|^2 \rangle}{\sqrt{\langle |V_n|^4 \rangle \ \langle |V_n(p)|^4 \rangle}}$$

- The **flow angle decorrelation** is obtained from the **ratio of the flow vector and flow magnitude** factorization coefficients,

$$F_n(p) = \frac{\langle V_n^2 V_n^*(p)^2 \rangle}{\langle |V_n|^2 |V_n(p)|^2 \rangle} = \frac{\langle |V_n|^2 |V_n(p)|^2 \cos[2n(\Psi_n - \Psi_n(p))] \rangle}{\langle |V_n|^2 |V_n(p)|^2 \rangle} \simeq \frac{\langle |V_n|^4 \cos[2n(\Psi_n - \Psi_n(p))] \rangle}{\langle |V_n|^4 \rangle}$$

# Model Results

(flow vector)$^2$-(flow vector)$^2$

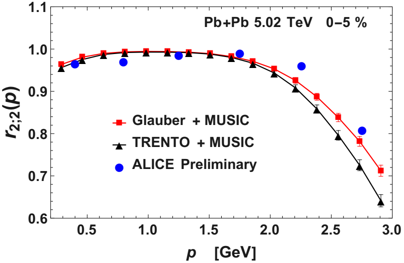


(flow magnitude)$^2$-(flow magnitude)$^2$

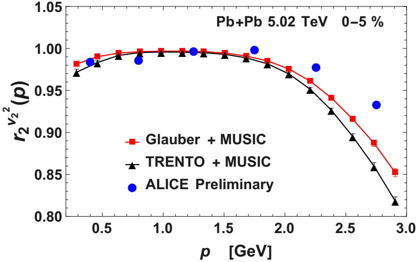


flow angle decor.

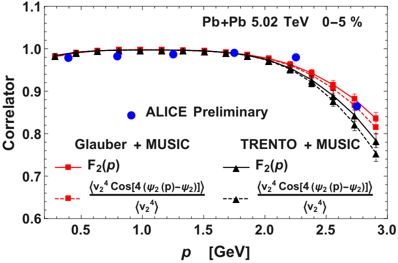


- **Similar momentum dependent correlations between mixed-flows e.g. $V_2^2 - V_4(p)$ and $V_2 V_3 - V_5(p)$** could be studied $\longrightarrow$ measure of **non-linear** medium response
- **For more detailed results and discussions, please follow the poster session.**

# Jet Energy Loss in Relativistic Heavy-Ion Collisions with Realistic Medium Modeling

Bc. Josef Bobek

Supervisor: Iurii Karpenko, Ph.D.

FNSPE CTU

# Heavy-Ion Collision

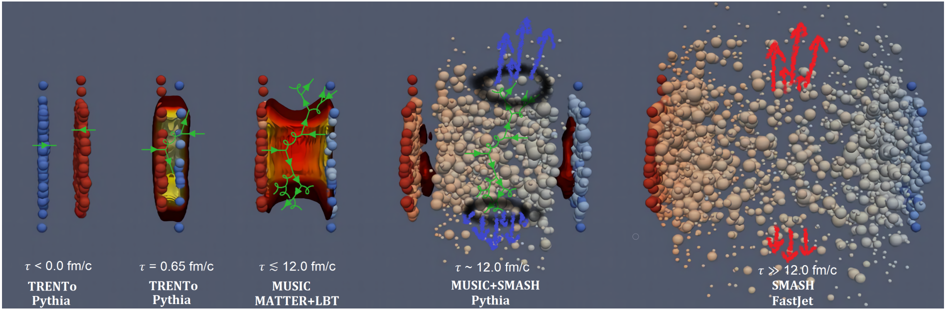

# Nuclear Modification Factor $R_{\mathrm{AA}}$ and Jet Shape $P(\Delta r)$ for Simplified (Brick) Medium

$$R_{\mathrm{AA}} = \frac{\frac{\mathrm{d}^2 N^{\mathrm{AA}}_{\mathrm{jet}}}{\mathrm{d}p_T \mathrm{d}y}}{\langle T_{\mathrm{AA}} \rangle \frac{\mathrm{d}^2 \sigma^{pp}_{\mathrm{jet}}}{\mathrm{d}p_T \mathrm{d}y}},$$

$$P(\Delta r) = \frac{1}{N_{\mathrm{jet}}} \frac{\mathrm{d}\left(p^i_{\mathrm{T}} - p^h_{\mathrm{T}}\right)}{\mathrm{d}z}$$

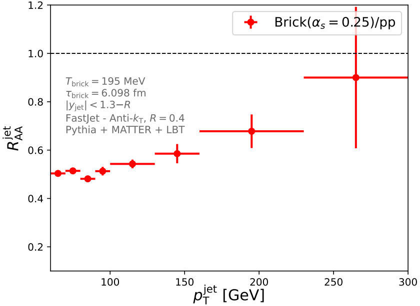


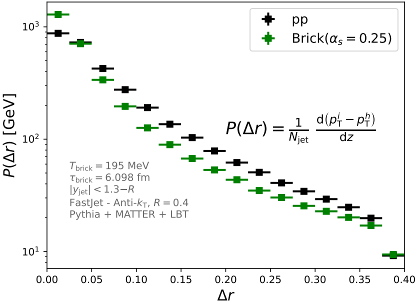

# Nuclear Modification Factor $R_{\mathrm{AA}}$ and Jet Shape $P(\Delta r)$ for Realistic Medium

$$R_{\mathrm{AA}} = \frac{\frac{\mathrm{d}^2 N_{\mathrm{jet}}^{\mathrm{AA}}}{\mathrm{d}p_T \mathrm{d}y}}{\langle T_{\mathrm{AA}} \rangle \frac{\mathrm{d}^2 \sigma_{\mathrm{jet}}^{pp}}{\mathrm{d}p_T \mathrm{d}y}},$$

$$P(\Delta r) = \frac{1}{N_{\mathrm{jet}}} \frac{\mathrm{d}\left(p_{\mathrm{T}}^{i} - p_{\mathrm{T}}^{h}\right)}{\mathrm{d}z}$$

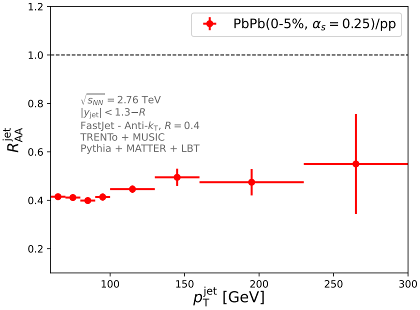


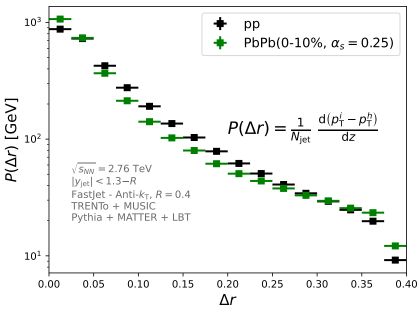

# THE DEVELOPMENT OF A MACHINE LEARNING-BASED HADRONIZATION MODEL

22nd ZIMÁNYI SCHOOL

WINTER WORKSHOP
ON HEAVY ION PHYSICS
5-9. 12. 2022.


**GÁBOR BÍRÓ**
biro.gabor@wigner.hu

Gergely Gábor Barnaföldi
Bence Tankó-Bartalis


arXiv:2111.15655
arXiv:2210.10548

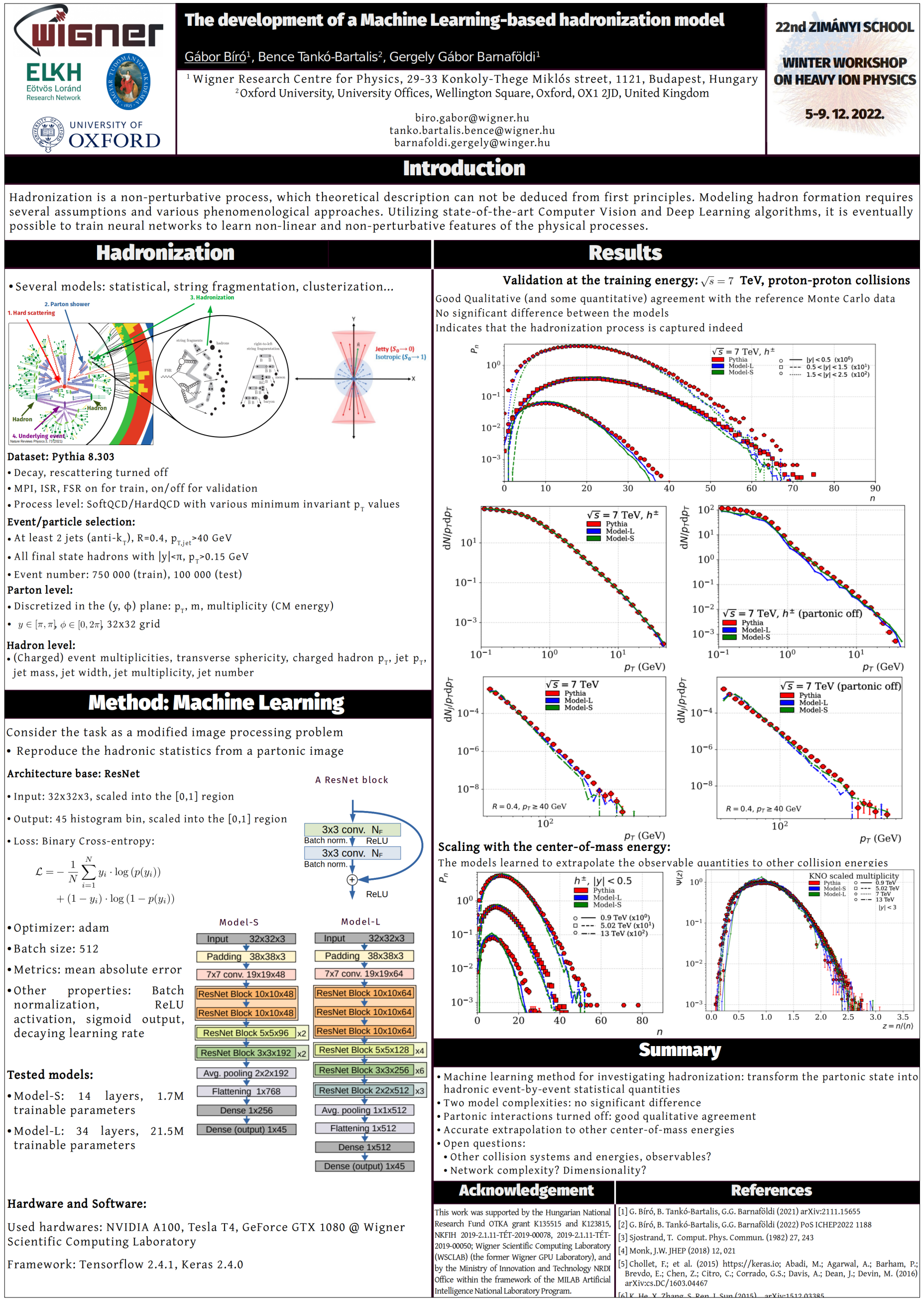

**The development of a Machine Learning-based hadronization model**


Gábor Bíró[1], Bence Tankó-Bartalis[2], Gergely Gábor Barnaföldi[1]

[1] Wigner Research Centre for Physics, 29-33 Konkoly-Thege Miklós street, 1121, Budapest, Hungary
[2] Oxford University, University Offices, Wellington Square, Oxford, OX1 2JD, United Kingdom

biro.gabor@wigner.hu
tanko.bartalis.bence@wigner.hu
barnafoldi.gergely@winger.hu


22nd ZIMÁNYI SCHOOL
WINTER WORKSHOP ON HEAVY ION PHYSICS
5-9. 12. 2022.

## Introduction

Hadronization is a non-perturbative process, which theoretical description can not be deduced from first principles. Modeling hadron formation requires several assumptions and various phenomenological approaches. Utilizing state-of-the-art Computer Vision and Deep Learning algorithms, it is eventually possible to learn non-linear and non-perturbative features of the physical processes.

## Hadronization

- Several models: statistical, string fragmentation, clusterization...

**Dataset: Pythia 8.303**
- Decay, rescattering turned off
- MPI, ISR, FSR on for train, on/off for validation
- Process level: SoftQCD/HardQCD with various minimum invariant $p_T$ values

**Event/particle selection:**
- At least 2 jets (anti-$k_T$), R=0.4, $p_{T,jet}$>40 GeV
- All final state hadrons with $|y|<\pi$, $p_T$>0.15 GeV
- Event number: 750 000 (train), 100 000 (test)

**Parton level:**
- Discretized in the (y, ϕ) plane: $p_T$, m, multiplicity (CM energy)
- $y \in [\pi,\pi]$, $\phi \in [0,2\pi]$, 32x32 grid

**Hadron level:**
- (Charged) event multiplicities, transverse sphericity, charged hadron $p_T$, jet $p_T$, jet mass, jet width, jet multiplicity, jet number

## Method: Machine Learning

Consider the task as a modified image processing problem
- Reproduce the hadronic statistics from a partonic image

**Architecture base: ResNet**
- Input: 32x32x3, scaled into the [0,1] region
- Output: 45 histogram bin, scaled into the [0,1] region
- Loss: Binary Cross-entropy:

$$\mathcal{L} = -\frac{1}{N}\sum_{i=1}^{N} y_i \cdot \log(p(y_i)) + (1-y_i)\cdot\log(1-p(y_i))$$

- Optimizer: adam
- Batch size: 512
- Metrics: mean absolute error
- Other properties: Batch normalization, ReLU activation, sigmoid output, decaying learning rate

**Tested models:**
- Model-S: 14 layers, 1.7M trainable parameters
- Model-L: 34 layers, 21.5M trainable parameters

**Hardware and Software:**

Used hardwares: NVIDIA A100, Tesla T4, GeForce GTX 1080 @ Wigner Scientific Computing Laboratory

Framework: Tensorflow 2.4.1, Keras 2.4.0

## Results

**Validation at the training energy: $\sqrt{s}=7$ TeV, proton-proton collisions**

Good Qualitative (and some quantitative) agreement with the reference Monte Carlo data
No significant difference between the models
Indicates that the hadronization process is captured indeed

**Scaling with the center-of-mass energy:**
The models learned to extrapolate the observable quantities to other collision energies

## Summary

- Machine learning method for investigating hadronization: transform the partonic state into hadronic event-by-event statistical quantities
- Two model complexities: no significant difference
- Partonic interactions turned off: good qualitative agreement
- Accurate extrapolation to other center-of-mass energies
- Open questions:
  - Other collision systems and energies, observables?
  - Network complexity? Dimensionality?

## Acknowledgement


This work was supported by the Hungarian National Research Fund OTKA grant K135515 and K123815, NKFIH 2019-2.1.11-TÉT-2019-00078, 2019-2.1.11-TÉT-2019-00050; Wigner Scientific Computing Laboratory (WSCLAB) (the former Wigner GPU Laboratory), and by the Ministry of Innovation and Technology NRDI Office within the framework of the MILAB Artificial Intelligence National Laboratory Program.


## References


[1] G. Bíró, B. Tankó-Bartalis, G.G. Barnaföldi (2021) arXiv:2111.15655
[2] G. Bíró, B. Tankó-Bartalis, G.G. Barnaföldi (2022) PoS ICHEP2022 1188
[3] Sjostrand, T. Comput. Phys. Commun. (1982) 27, 243
[4] Monk, J.W. JHEP (2018) 12, 021
[5] Chollet, F.; et al. (2015) https://keras.io; Abadi, M.; Agarwal, A.; Barham, P.; Brevdo, E.; Chen, Z.; Citro, C.; Corrado, G.S.; Davis, A.; Dean, J.; Devin, M. (2016) arXiv:cs.DC/1603.04467
[6] K. He, X. Zhang, S. Ren, J. Sun (2015) arXiv:1512.03385

# Hadronization with Machine Learning

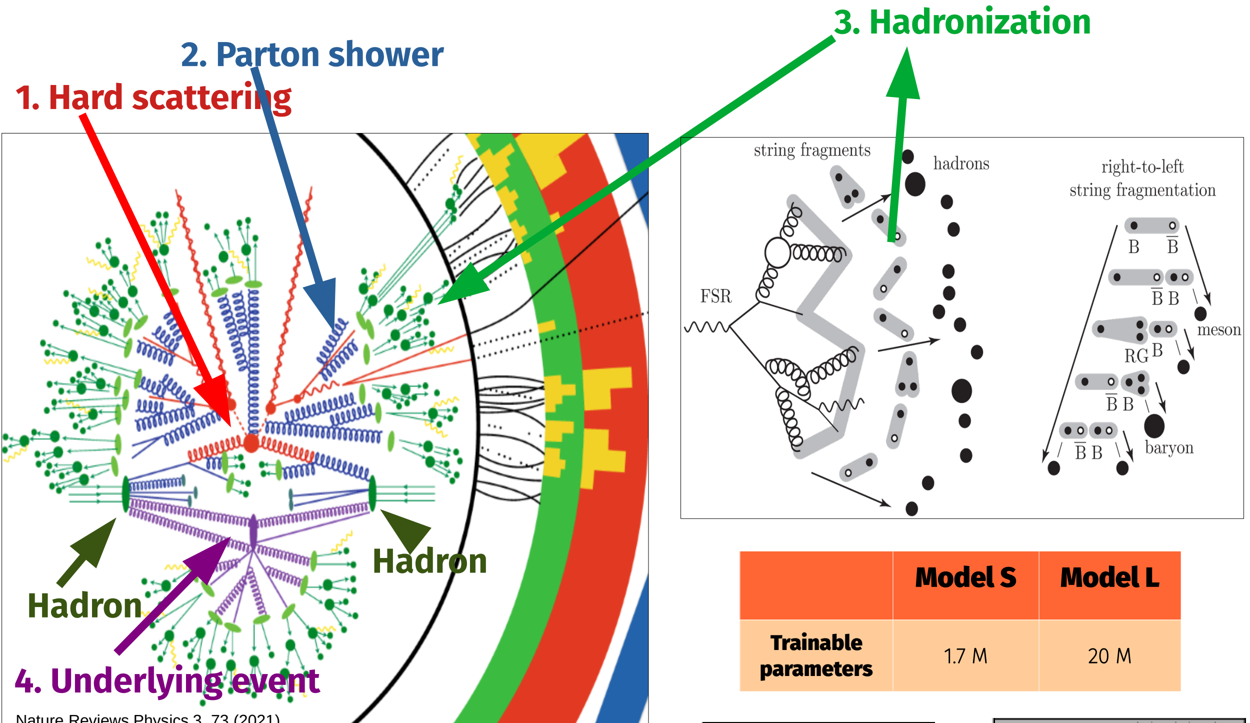


## Input:

Parton level

Discretized in the $(y, \phi)$ plane: $p_T$, m, multiplicity

$y \in [\pi, \pi]$ 32 bins

$\phi \in [0, 2\pi]$ 32 bins

## Hadron level output:

(Charged) event multiplicity, (tr-)sphericity, mean jet $p_T$, -mass, -width, -multiplicity

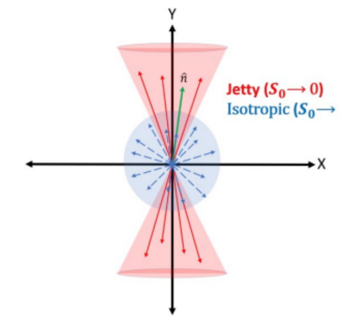


| | Model S | Model L |
|---|---|---|
| Trainable parameters | 1.7 M | 20 M |

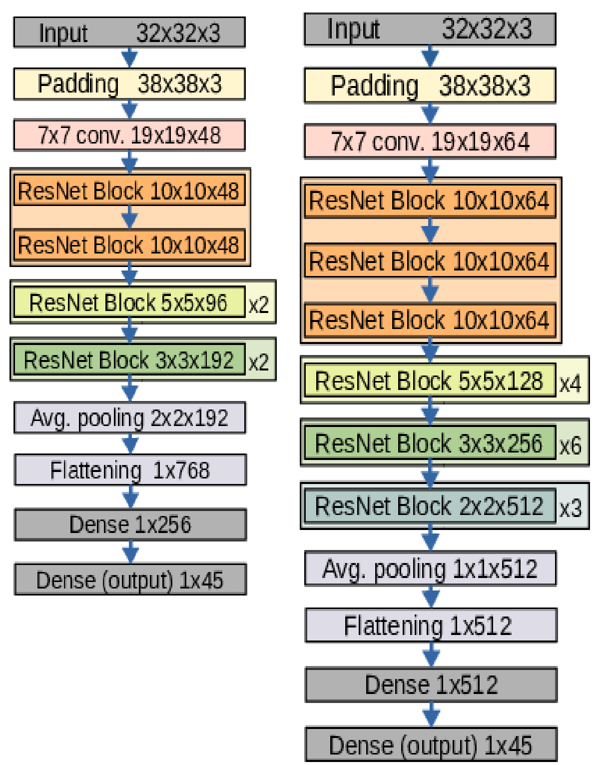


## ResNet blocks:

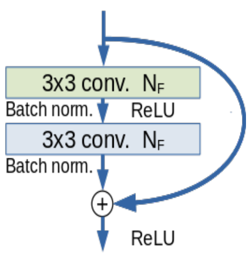


Used hardwares: Nvidia Tesla T4, GeForce GTX 1080 @ Wigner Scientific Computing Laboratory

Framework: Tensorflow 2.4.1, Keras 2.4.0

## Monte Carlo data: Pythia 8.303

Monash tune

Rescattering and decays turned off

ISR, FSR, MPI: turned on

Selection:

- All final particles with $|y| < \pi$
- At least 2 jets
  - Anti-$k_T$
  - R=0.4
  - $p_T$>40 GeV

Event number:

- Train: 750 000, $\sqrt{s}$ = 7 TeV
- Validation and test: 100 000
- ~20 GB raw data

# pp @ LHC, Training, validation and predictions

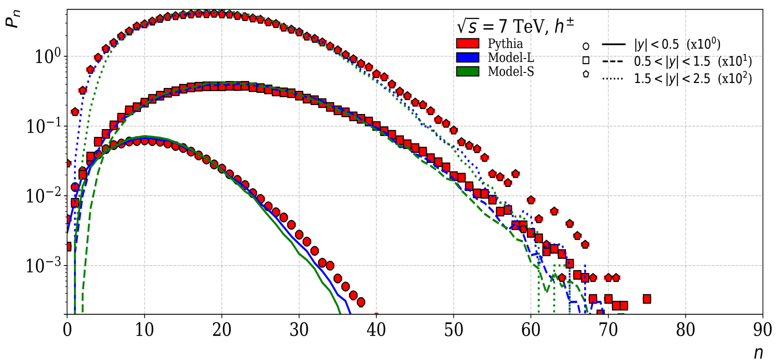


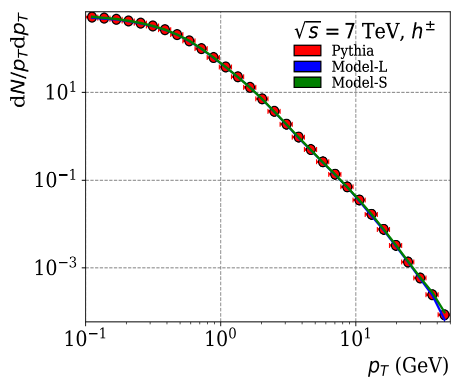


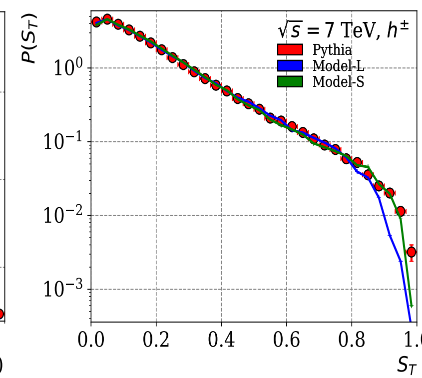


Charged hadron multiplicity at various rapidity windows

**Good agreement for both models**

Charged hadron transverse momentum
0.1 GeV ≤ pT ≤ 50 GeV

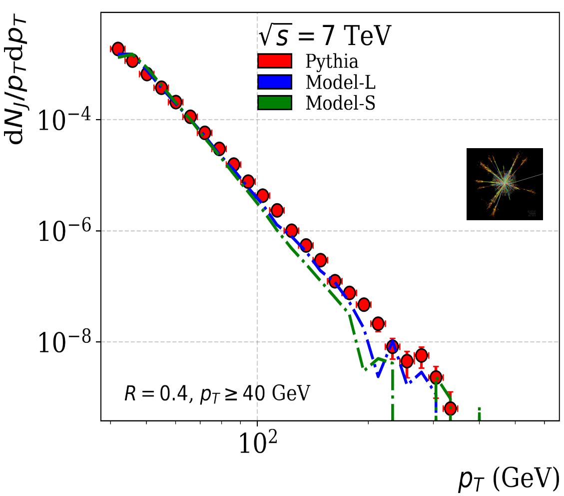


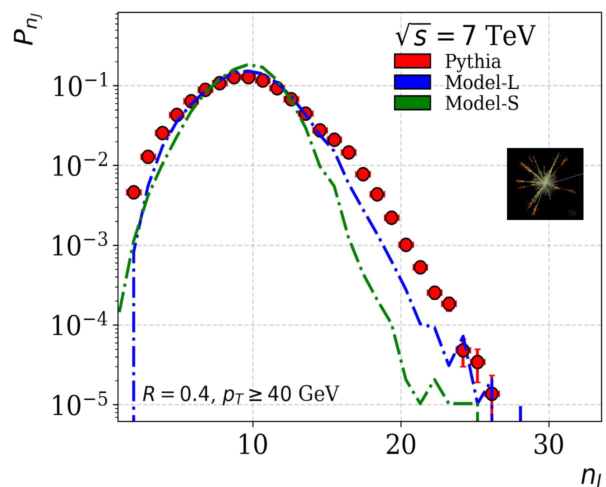


Jets:

- Mean $p_T \leq 400$ GeV
- Mean multiplicity

**The smaller model performs better**

**Training only at a single c.m. energy, predictions at other energies**

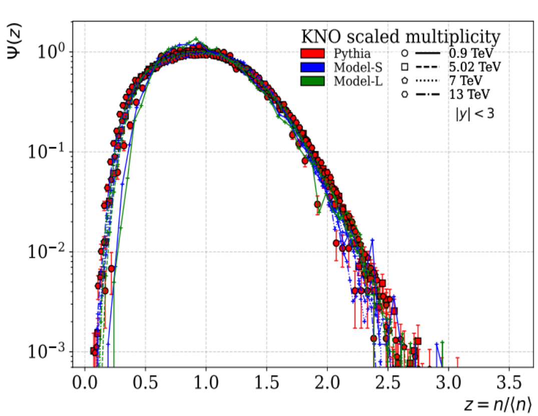


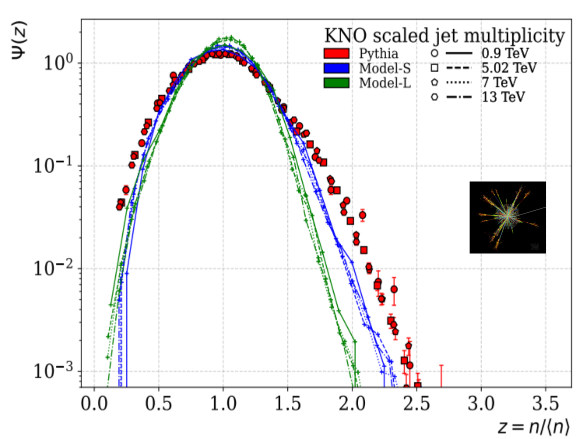


Scaling function for multiplicities at various energies:

$$P_n = \frac{1}{\langle n \rangle} \Psi\left(\frac{n}{\langle n \rangle}\right)$$

Charged hadron multiplicities in **jetty** events: good overlap and agreement at **all LHC energies**

Mean jet multiplicities: different scaling for the models

# The STAR Event Plane Detector

22nd Zimányi School Winter Workshop

- Much higher granularity compared to BBC
  - BBC: 36 tiles (only 18 inner used) ⇒ EPD: 372 tiles
  - Also larger acceptance: [3.3,5.0] ⇒ [2.1,5.1]
  - 16 radial segments (rings)
  - 24 azimuthal segments (sectors)
- Radial segmentation driven by flow, vertex, trigger
- Azimuthal segmentation driven by higher-order flow harmonics
- Each tile registers hits, mostly MIPs
  - Landau distribution of a single hit
  - Convolution for multiple hits
  - Poisson distribution of MIP weights

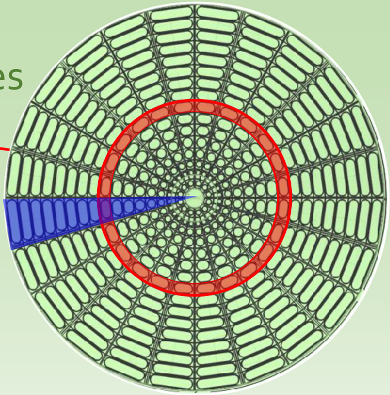

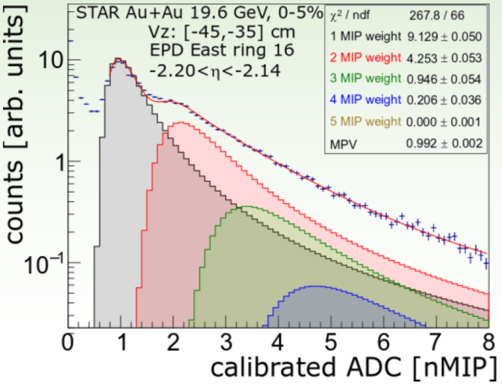

# The EPD Response Matrix

22nd Zimányi School Winter Workshop

- Use iterative unfolding, based on G. D'Agostini, Nucl. Instr. Meth. A362 (1995) 487
- Implemented in RooUnfold, response matrix to be calculated as:

```
for(PrimaryTracks)
{
  if(no EPD hits from that Primary Track)
  {
    R->Miss(TrackEta); //This track "missed" the EPD
  }
  else
  {
    for(EPD hits of that Primary Track)
    {
      R->Fill(EPDRingNumber,TrackEta);
    }
  }
}
```

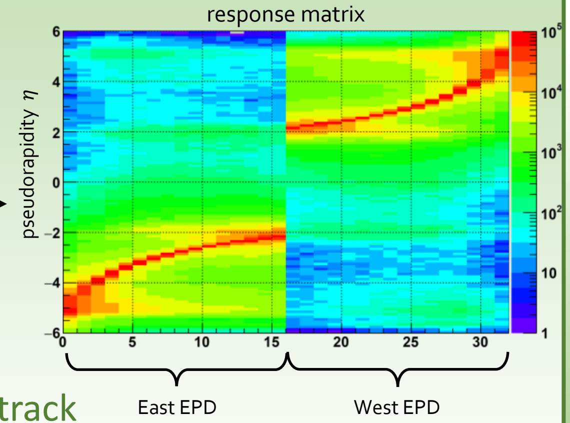


- In the simulation, we need:
  - list of **primary tracks**
  - list of **EPD hits**, associated to the primary track
- The above is possible in HIJING+GEANT simulation
  - Note: no (light) ion fragments in HIJING; note PHOBOS paper Phys.Rev.C 94 (2016) 024903

# Results & Systematics



- Systematic checks in the unfolding
  - Determination of the longitudinal vertex position (±5 cm shift) & centrality (±5% change)
  - Comparison of several vertex intervals (+40 cm and -40 cm from geometric center)
  - Unfolding method:
    1. Unfolding $dN/d\eta$; correcting via $N_{ch}(\eta)/N_{tot}(\eta)$ from HIJING
    2. Correcting via $N_{ch}(i_{ring})/N_{tot}(i_{ring})$; unfolding "corrected" EPD distribution
    3. Use RooUnfold's "Fakes" (where neutrals ⇔ "fake" hits)
  - Change in charged/neutral ratio in the training sample (±15%)
  - Change in transverse momentum slope in the training sample
  - Change in $dN/d\eta$ of training sample
    - Broadening to $\Delta\eta = 10$, tightening to $\Delta\eta = 2$
    - Shifting by ±3 units of rapidity
- EPD: number of MIPs ≤ 5, more systematic checks to be done
- Discrepancy with PHOBOS: several differences, multiple reasons possible
  - Unfolding vs correction, segmentation, simulation imperfection, neglections in raw signal

Results

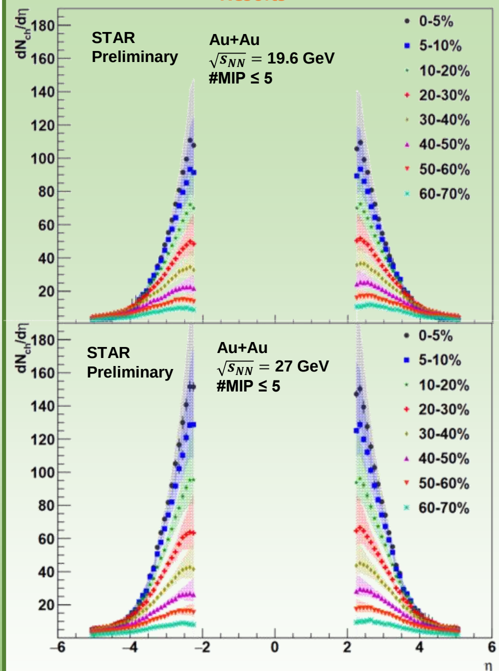


- Results obtained for 19.6 GeV and 27 GeV
- Via HIJING+GEANT, without ion fragments
- EPD range: $2.14 < |\eta| < 5.09$
- Expected $\eta$, centrality, $\sqrt{s_{NN}}$ dependence

# Newtonian noise estimation for Einstein Telescope – the effect of rock rheology

Tamás FÜLÖP[1,2], László KOVÁCS[3], Róbert KOVÁCS[1,2,4], Mátyás SZÜCS[1,2,4], Donát M. TAKÁCS[1,2], Péter VÁN[1,2,4]

[1]Budapest University of Technology and Economics, [2]Montavid Thermodynamics Research Group, [3]ROCKSTUDY Ltd., [4]Wigner Research Centre for Physics

8st December, 2022

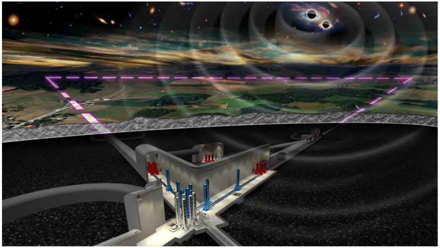

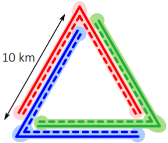


- Einsteint telescope – increased sensitivity $\Longrightarrow$ distinguishing, separation and mitigation of noises are crucial
- Newtonian noise – existing calculations based on elasticity
- Rocks perform rheological (viscoelastic) behaviour – how to predict its effects?
- Commercial finite element softwares $\Longrightarrow$ not reliable enough
- Self-developed thermodynamically consistent symplectic-based finite difference method

**Thank you for your attention!**

# Probability density-based image reconstruction for proton Computed Tomography

Ákos Sudár [1,2]
and Gergely Gábor Barnaföldi [1]
[1] Wigner Research Centre for Physics
[2] Budapest University of Technology and Economics

on behalf of Bergen proton CT collaboration
(full collaboration list)

Zimányi Winter School 2022,
8 Dec 2022

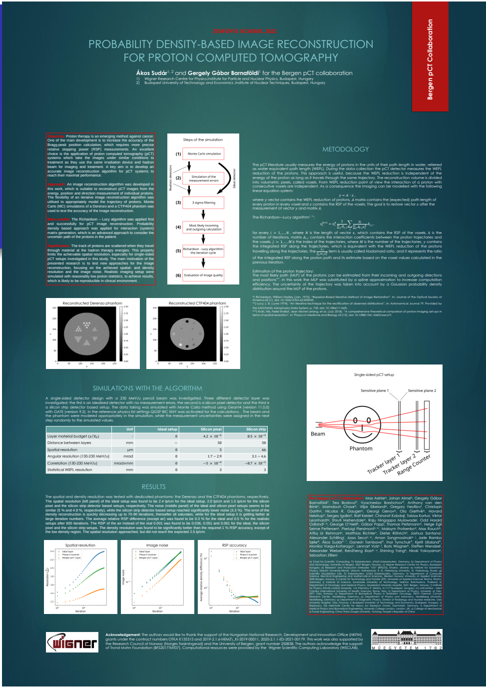

Novel points:

- Richardson – Lucy algorithm (first applied for pCT)
- Probability-density based trajectory model
- Measurement uncertainties in most likely path calculations

Single-sided setup:

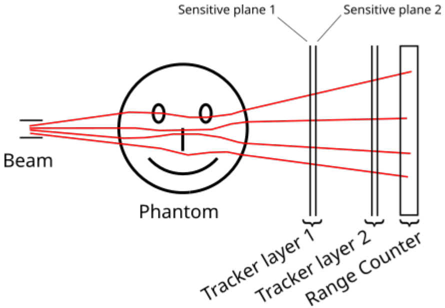


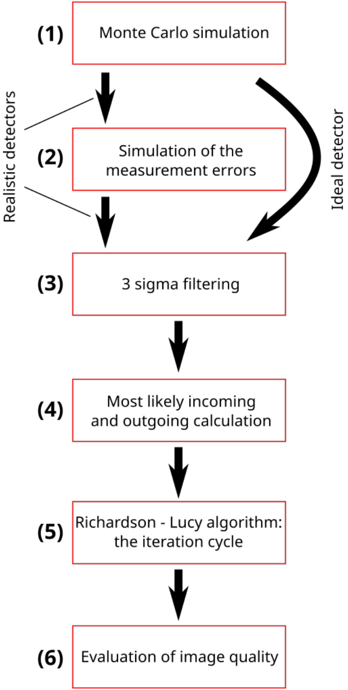

Results:

- Spatial resolution ($MTF_{10\%}$):
  ideal: 2.4 lp/cm & realistic: 2.0 lp/cm
- Relative stopping power (RSP) accuracy:
  0.3 % for ideal & 0.5 % for realistic setup
- Image noise: around 5 % for both cases

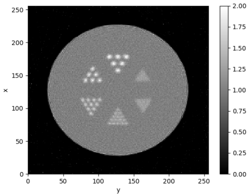


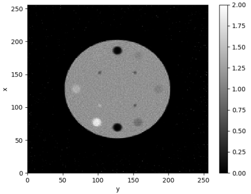


## Spatial resolution

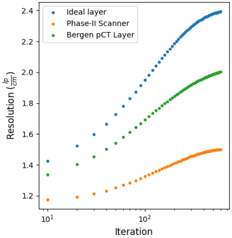


## RSP accuracy

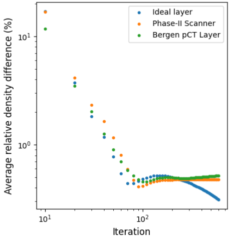


**Acknowledgement:** The authors would like to thank the support of the Hungarian National Research, Development and Innovation Office (NKFIH) grants under the contract numbers OTKA K135515 and 2019-2.1.6-NEMZ_KI-2019-00011, 2020-2.1.1-ED-2021-00179. This work was also supported by the Research Council of Norway (Norges forskningsrad) and the University of Bergen, grant number 250858. The authors acknowledge the support of Trond Mohn Foundation (BFS2017TMT07). Computational resources were provided by the Wigner Scientific Computing Laboratory (WSCLAB).

# Contributions of gravitational-wave observations to heavy-ion physics

**Edit Fenyvesi**
Institute for Nuclear Research (Atomki), Debrecen, Hungary; Wigner Research Centre for Physics, Budapest, Hungary

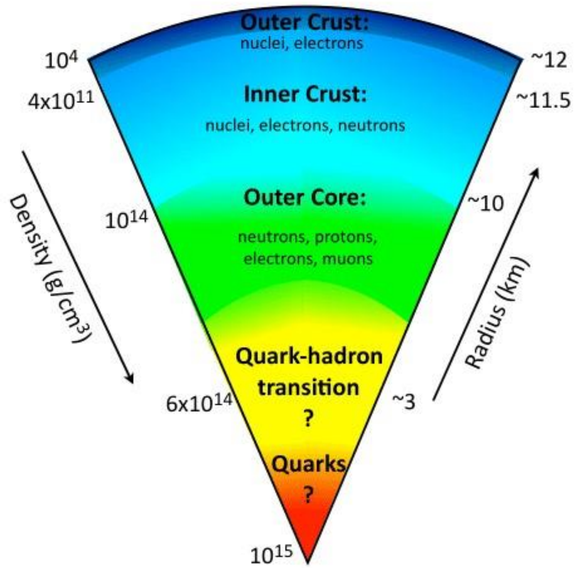


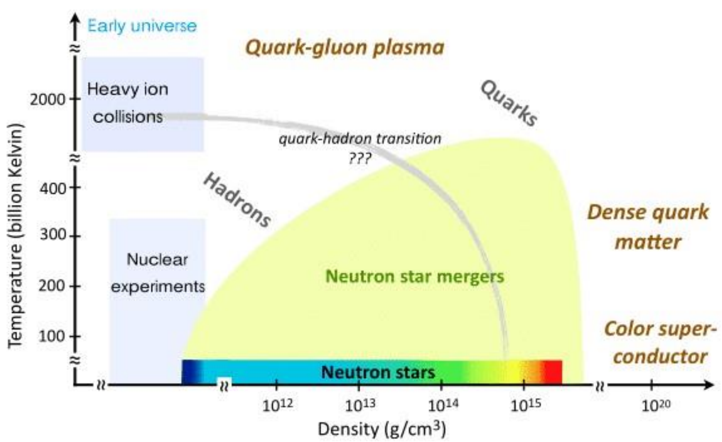


Left: Conjectured interior structure of a **neutron star** [1].

Right: Matter encountered in neutron stars and binary mergers explores a large part of the QCD phase diagram in regimes that are inaccessible to terrestrial collider experiments [1].

# Gravitational-wave detectors

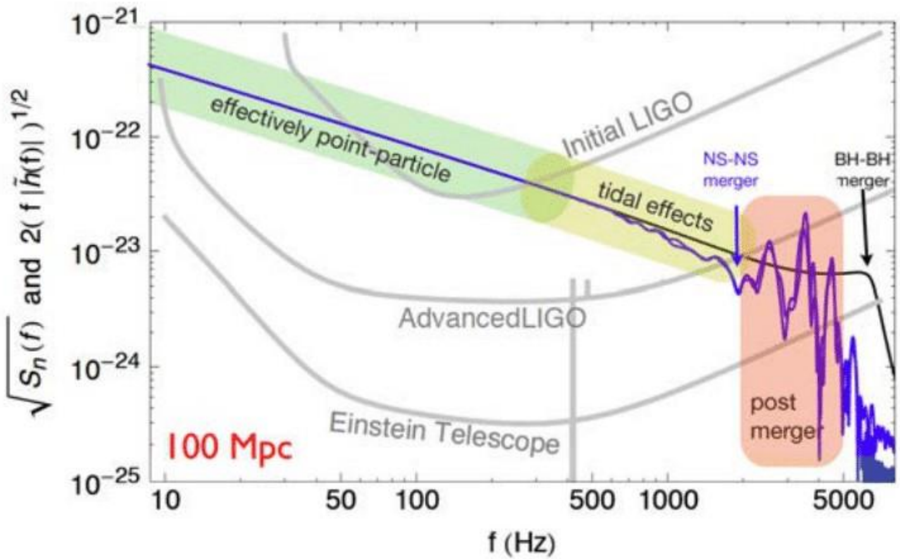


Gravitational-wave signal from a NS-NS merger at a distance 100 Mpc, as it sweeps across the detector-accessible frequency range [1].

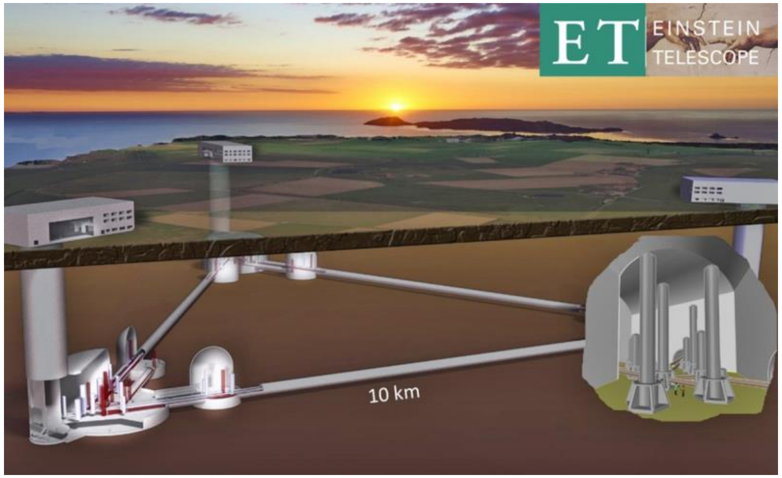


Einstein Telescope

# Merging nuclear theory, multi-messenger astrophysics and data from HIC experiments

- According to a recently published study, new constraints on the EOS above 1 $n_{sat}$ was given by merging theoretical computations, results of heavy-ion collision (HIC) experiments and GW signals together with other multi-messenger astronomy observations of neutron stars [3].
- At first, 15000 different EOS were created in a way that they span the theoretical uncertainty range of the chiral effective field theory calculations.
- The GW170817 signal was compared to theoretical GW models depending on the features of NSs. This way, constraint on maximum mass of NSs could be made, which resulted in greater accuracy of the EOS.
- The Einstein Telescope is expected to detect GW signals of $7 \times 10^4$ neutron star mergers per year, therefore different parameters of NSs could be examined with increased accuracy.
- This way, improved EOS could be determined in the $n_{sat}$ range where theoretical calculations become less reliable.
- Moreover, EOS of the matter arises after the coalescence of NSs could be known better by being able to detect the GW signal of the post-merger phase.

**References:**
[1] ET Steering Committee Editorial Team,Design Report Update 2020 for the Einstein Telescope., https://gwic.ligo.org/3Gsubcomm/docs/ET-0007B-20_ETDesignReportUpdate2020.pdf
[2] LIGO-Virgo Compact Binary Catalogue., https://catalog.cardiffgravity.org/
[3] S. Huth, P.T.H. Pang, I. Tews, et al., Constraining neutron-star matter with microscopic and macroscopic collisions., Nature 606, 276–280 (2022). doi:10.1038/s41586-022-04750-w. https://doi.org/10.1038/s41586-022-04750-w

# IF A SCALAR FIELD IS INTRODUCED AS A THERMODYNAMIC STATE VARIABLE, THEN THE SECOND LAW OF THERMODYNAMICS CONSTRAINS THE FIELD TO BE ONLY GRAVITY.

Máté Pszota, Peter Ván and Sumiyoshi Abe

Thermodynamic modified gravity and dark matter

*poster*

$$\Delta\varphi = 4\pi G\rho + K(\nabla\varphi)^2$$

$$\varphi_{vacuum}(r) = \frac{1}{K}\ln\frac{r}{K + Cr} + \varphi_0$$

The obtained field equation includes an additional square gradient term, resulting in a modified vacuum potential.

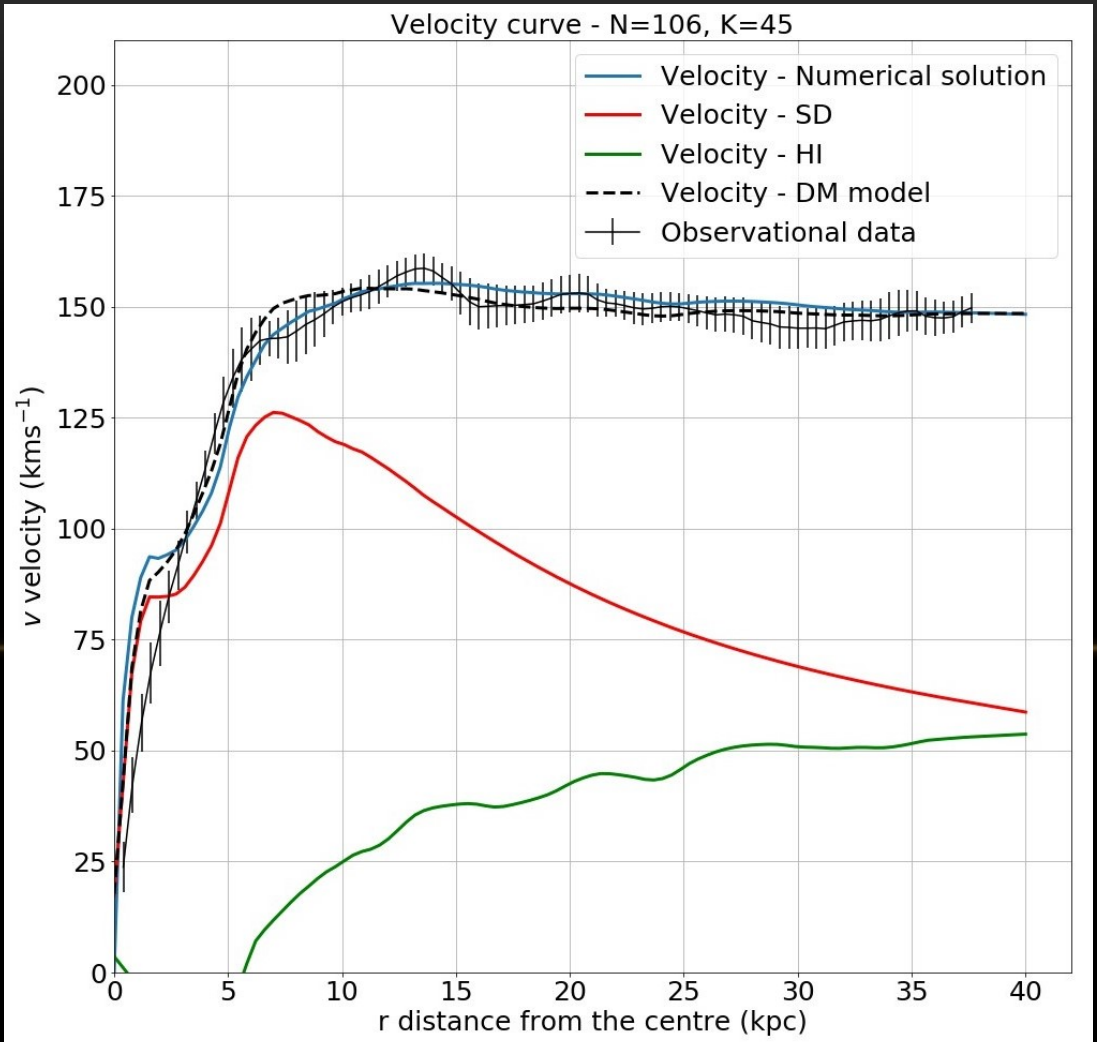


The solution with galactic density distribution is similar to dark matter.

# Exploring Quantum Entanglement in Heavy Ion Collisions

Eliana Marroquin[1] and Marcelo Munhoz[1]

[1]High Energy Physics and Instrumentation Center (HEPIC), Physics Institute at the University of São Paulo, Brazil

## Perturbative QCD

Recent studies established the relation between entanglement entropy $S(x)$ and parton densities for small Bjorken-x, large rapidity regime

$$S_{parton} = \ln(xG(x;Q^2) + x\Sigma(x;Q^2))$$

initial state

[1] Phys. Rev. D 95, 114008. D. Kharzeev and E. Levin (2017)
[2] Phys. Rev. D 104, 031503. D. Kharzeev and E. Levin (2021)

## Entanglement Entropy

Entanglement entropy (EE) applies to both perturbative and non-perturbative regimes

→ EE can connect initial and final state of high-energy reactions

$$S_{hadron} = -\sum P(N) \ln P(N)$$

final state

## High Energy Processes

Try to verify the relation: $S_{parton} \leq S_{hadron}$

1. Deep Inelastic Scattering [3] arXiv:2207.09430v1. M. Hentschinski et al (2022)
2. Proton-proton collisions [4] Phys. Rev. Lett. 124, 062001. Z. Tu et al (2020)

**Our proposal: entanglement in proton-nucleus collisions with ALICE**

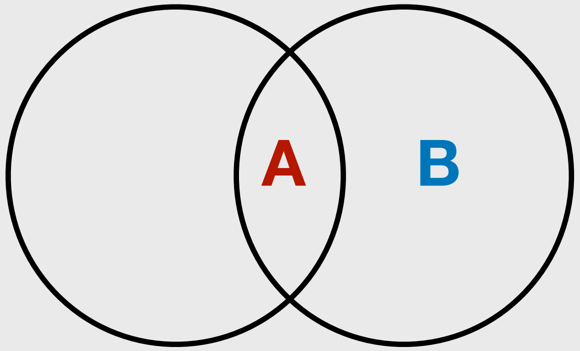

# Entanglement in proton-proton collisions

## Charged-particle multiplicity distributions

- *Multiplicity distribution* is the probability distribution $P(N_{ch})$ of a collision event to have $N_{ch}$ particles produced
- [4]: proton-proton (pp) collisions with center-of-mass energies $\sqrt{s} = 0.9$ , $2.36$ , and $7$ TeV at different pseudo-rapidity ranges $|\eta| < 0.5$, $1.0$, and $1.5$ of the CMS experiment
- Using Negative Binomial Distribution (NBD) and double NBD to fit the data, we take as our distribution $P(N)$ half of the average to account for one proton distribution

## Parton Distribution Functions

- The measurable cross-section can be factorized in a short-distance interaction — the partonic cross-section — and in a function containing the long-distance interactions, the Parton Distribution Functions (PDFs)
- PDFs cannot be derived from first principles → global QCD analysis procedure
- pp analysis: used HERAPDF, NNPDF, and MSTW sets to calculate $S_{parton}$ for d, u, s, and the gluon distribution

# Entanglement entropies for pp collisions

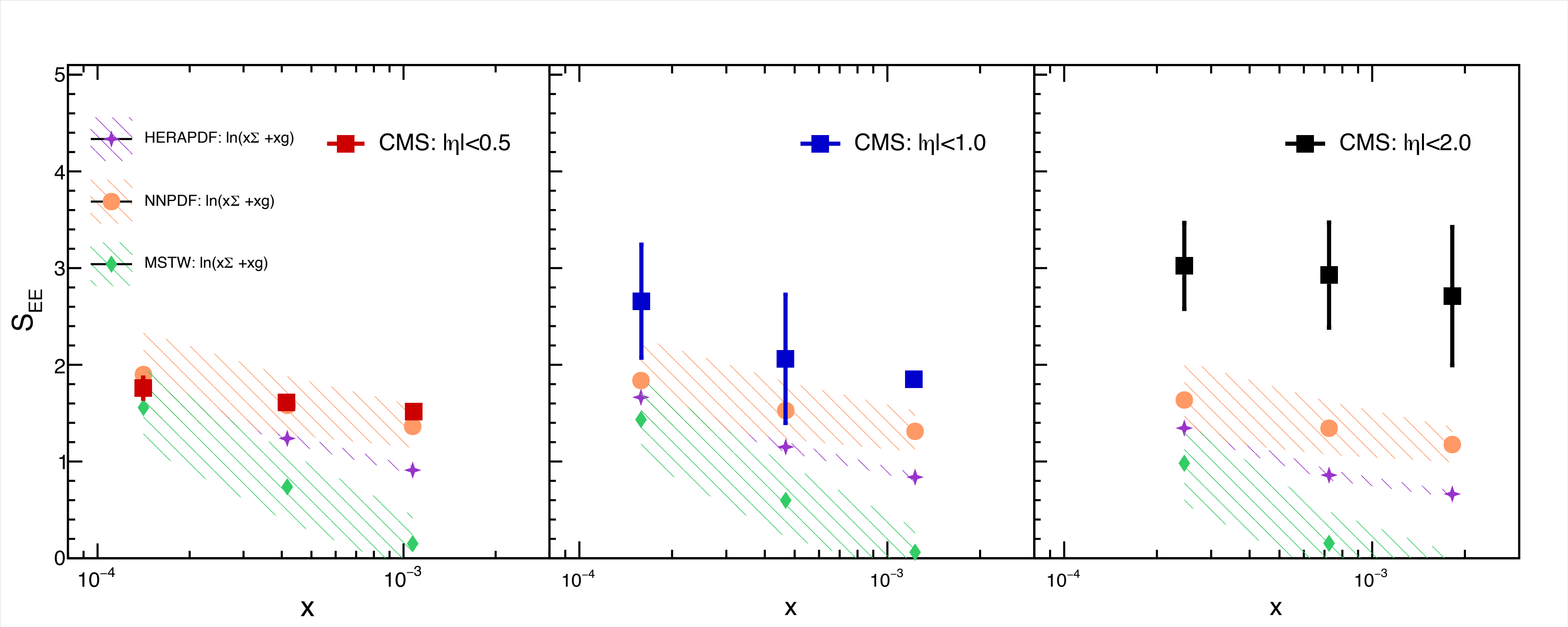


# What about proton-nucleus collisions?

- **Final state entropy** Currently working on the data analysis of charged-particle distributions of proton-Lead collisions with ALICE [PAG-MM: https://indico.cern.ch/event/1214899/]
- **Initial state entropy** nPDFs: Fewer data constraints lead to parametrization bias → new approaches for $S_{parton}$

**This work is supported by The São Paulo Research Foundation (FAPESP), grant numbers: 2020/04438-7 and 2022/05642-0.**

# Effect of Glueball scattering on the GRG

Enrico Trotti

(in collaboration with Shahriyar Jafarzade and Francesco Giacosa)

Poster based on: E. Trotti, S. Jafarzade, F. Giacosa, Thermodynamics of the GRG, arXiv:2212.03272 .

Zimanyi Winter School, 5-9 December 2022

Jan Kochanowski University, Kielce, Poland

December 8, 2022

- Glueball Resonance Gas (GRG): gas of glueballs $\rightarrow$ thermal properties of YM ($T < T_C$): *pressure*, *entropy* & *trace anomaly*
- In YM, the low-mass glueballs are stable.

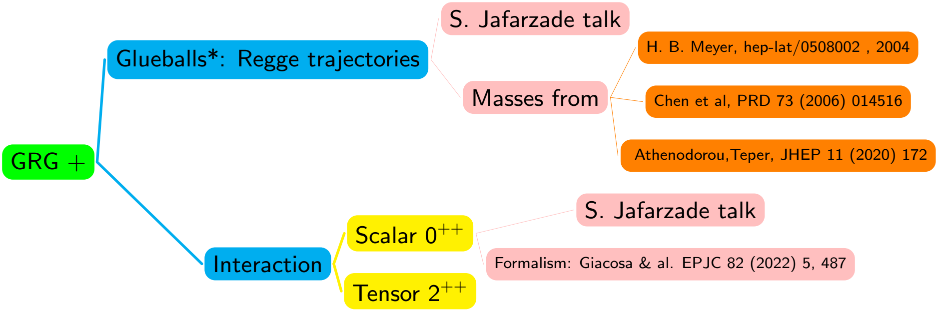


$$p^{\text{int}}_{J^{PC}} = -T \sum_J (2J+1) \sum_{l=0}^{\infty} \int_0^{\infty} dx \frac{2l+1}{\pi} \frac{d\delta_l^J(x^2)}{dx} \int \frac{d^3k}{(2\pi)^3} \ln\left(1 - e^{-\beta \frac{\sqrt{k^2+x^2}}{T}}\right)$$

## Scalar interaction $|J, m\rangle \longrightarrow J = 0, m = 0$

1 amplitude →1 phase shift →1 pressure contribution

## Tensor interaction $|J, m\rangle \longrightarrow J = 2, m \in [-2, 2]$

~~625 amplitudes~~ →25 non-zero amplitudes →25 phase shifts →25 pressure contributions
(detailed calculation during poster session)

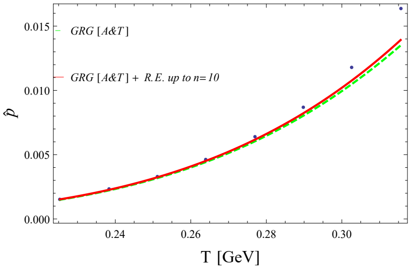


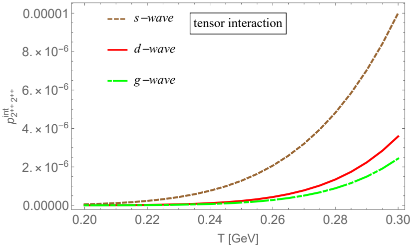


Point data from Borsányi & al. (2012) JHEP, 07, 056

# Conclusions

- Free glueball gas with 10-15 lightest state: sufficient for TMD description of LQCD results for pure YM.
- The critical temperature in YM turns out to be $T_C = 323 \pm 18$ MeV.
- Effect of excited glueballs via Regge trajectories and effect of interaction are very small.
- GRG works well with the masses of Athenodorou & Teper $\rightarrow$ those masses are favoured.

# Superfluid thermodynamics

Peter Ván

Wigner Research Centre for Physics
Institute of Particle and Nuclear Physics,
Department of Theoretical Physics
and
BME, Department of Energy Engineering

Zimányi Winter School, 2022.

# Quantum to fluid

## Connected realities

quantum mechanics $\rightarrow$ *superfluids* $\rightarrow$ capillary fluids

## From special to general. Analogy?

$$i\hbar\partial_t\Psi + \frac{\hbar^2}{2m}\Delta\Psi - \Phi\Psi = 0,$$

Madelung transformation

$$\Psi = Re^{i\frac{\hbar}{m}S}.$$

$\rho = |\Psi|^2$, $\boldsymbol{v} = \nabla S$, fluid form:

$$\dot{\rho} + \rho\nabla\cdot\boldsymbol{v} = 0, \qquad \rho\dot{\mathrm{v}} + \nabla\cdot\boldsymbol{P_K}(\rho, \nabla\rho, \nabla^2\rho) = \mathbf{0},$$

Perfect Korteweg fluids.

# Fluid to quantum

## Thermodynamic deduction

capillary fluids $\Longrightarrow$ *superfluids* $\Longrightarrow$ quantum mechanics

## Consequences

- Second Law instead of variational principles
- Second Law instead of holography

A superfluid is not water with zero viscosity.
What about QGP?

# Finite volume effects on the QCD phase diagram: Importance of the vacuum size

Győző Kovács
PhD student
Eötvös University
Wigner RCP
kovacs.gyozo@wigner.hu

Zimányi School 2022
Poster Session
2022 December 8

Collaborators:
Péter Kovács, Wigner RCP
György Wolf, Wigner RCP
Pok Man Lo, Wroclaw U
Krzystof Redlich, Wroclaw U

The volume dependence of the phase diagram was studied in an (axial-)vector meson extended Polyakov quark-meson model via a low momentum cutoff.

- Restriction in momentum space
  = low momentum cutoff
- Applied to the fermion integrals
- Modification of vacuum contribution
  ⇒ change of phys. quantities
- Modification of thermal contribution

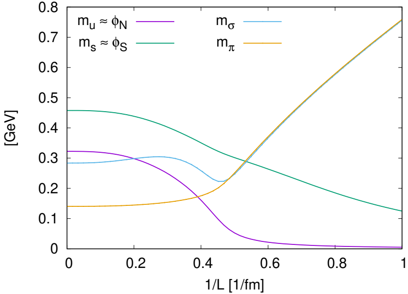

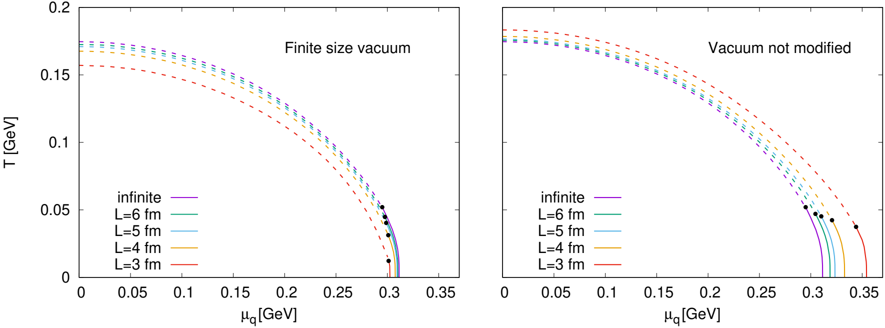


**For more details and further results find me in the poster section.**

# Isospin breaking in the EL$\sigma$M model

Péter Kovács, György Wolf - Wigner RCP

How well one can describe isospin breaking in a chiral meson model?

We use a Lagrangian that has global $U(3)_L \times U(3)_R$ chiral symmetry – like in QCD if the quark masses are zero – plus explicit symmetry breaking terms

$U(3)_L \times U(3)_R \simeq U(3)_V \times U(3)_A = SU(3)_V \times SU(3)_A \times U(1)_V \times U(1)_A$

$U(1)_V \longrightarrow$ baryon number conservation (exact symmetry of nature)

$U(1)_A \longrightarrow$ connected to axial anomaly

$SU(3)_A \longrightarrow$ broken down by any quark mass

$U(3)_L \times U(3)_R \longrightarrow$ broken to $U(1)_V \times SU(2)_V$ if $m_u = m_d \neq m_s$ (isospin symm.)
$\longrightarrow$ or to $U(1)_V$ if $m_u \neq m_d \neq m_s$ (realized in nature)

# Particle content

- Vector and Axial-vector meson nonets

$$V^\mu = \frac{1}{\sqrt{2}}\begin{pmatrix} \frac{\omega_N+\rho^0}{\sqrt{2}} & \rho^+ & K^{\star+} \\ \rho^- & \frac{\omega_N-\rho^0}{\sqrt{2}} & K^{\star0} \\ K^{\star-} & \bar{K}^{\star0} & \omega_S \end{pmatrix}^\mu \quad A^\mu = \frac{1}{\sqrt{2}}\begin{pmatrix} \frac{f_{1N}+a_1^0}{\sqrt{2}} & a_1^+ & K_1^+ \\ a_1^- & \frac{f_{1N}-a_1^0}{\sqrt{2}} & K_1^0 \\ K_1^- & \bar{K}_1^0 & f_{1S} \end{pmatrix}^\mu$$

$\rho \to \rho(770), K^\star \to K^\star(894)$
$\omega_N \to \omega(782), \omega_S \to \phi(1020)$

$a_1 \to a_1(1230), K_1 \to K_1(1270)$
$f_{1N} \to f_1(1280), f_{1S} \to f_1(1426)$

- Scalar ($\sim \bar{q}_i q_j$) and pseudoscalar ($\sim \bar{q}_i\gamma_5 q_j$) meson nonets

$$S = \frac{1}{\sqrt{2}}\begin{pmatrix} \frac{\sigma_N+a_0^0}{\sqrt{2}} & a_0^+ & K_0^{\star+} \\ a_0^- & \frac{\sigma_N-a_0^0}{\sqrt{2}} & K_0^{\star0} \\ K_0^{\star-} & \bar{K}_0^{\star0} & \sigma_S \end{pmatrix} \quad P = \frac{1}{\sqrt{2}}\begin{pmatrix} \frac{\eta_N+\pi^0}{\sqrt{2}} & \pi^+ & K^+ \\ \pi^- & \frac{\eta_N-\pi^0}{\sqrt{2}} & K^0 \\ K^- & \bar{K}^0 & \eta_S \end{pmatrix}$$

multiple possible assignments
mixing in the $\sigma_N - \sigma_S$ sector

$\pi \to \pi(138), K \to K(495)$
mixing: $\eta_N, \eta_S \to \eta(548),\ \eta'(958)$

If $\zeta_{N/S/3} \neq 0 \longrightarrow$ chiral symmetry is explicitly broken,
especially if $\zeta_3 \neq 0$ – and also $\delta_3 \equiv \delta_u - \delta_d \neq 0$ – the isospin symmetry is violated
Consequently nonzero vev for scalar-isoscalar fields: $\phi_{N/S} \equiv \langle\sigma_{N/S}\rangle$ and $\phi_3 \equiv \langle a_0^0\rangle$

$$\sigma_{N/S} \quad\to\quad \phi_{N/S} + \sigma_{N/S},\ a_0^0 \to \phi_3 + a_0^0.$$

Different particle mixings appear:

- mixings between nonets $V^\mu \longleftrightarrow S$ and $A^\mu \longleftrightarrow P$
- $N-3$ sectors of $V^\mu$ and $A^\mu$
- $N-3-S$ sectors of $S$ and $P$

# Determination of the parameters

There are 21 unknown parameters:
$m_0^2$, $m_1^2$, $c_1$, $\delta_S$, $\delta_3$, $g_1$, $g_2$, $\phi_N$, $\phi_S$, $\phi_3$, $\lambda_1$, $\lambda_2$, $h_1$, $h_2$, $h_3$, $m^2_{\mathrm{em},S}$, $m^2_{\mathrm{em},P}$, $m^2_{\mathrm{em},V}$, $m^2_{\mathrm{em},A}$, $\delta m_V^2$, $\delta m_A^2$ $\longrightarrow$ determined by the min. of $\chi^2$:

$$\chi^2(x_1,\ldots,x_N) = \sum_{i=1}^{M}\left[\frac{Q_i(x_1,\ldots,x_N) - Q_i^{\mathrm{exp}}}{\delta Q_i}\right]^2,$$

$(x_1,\ldots,x_N) = (m_0,\lambda_1,\lambda_2,\ldots)$, $Q_i(x_1,\ldots,x_N) \to$ calc. in the model, $Q_i^{\mathrm{exp}} \to$ PDG value,
$\delta Q_i =$ error (e.g. $\max\{5\%, \text{PDG value}\}$) multiparametric minimalization $\longrightarrow$ MINUIT

- PCAC $\to$ 2 physical quantities: $f_\pi, f_K$
- Charged and neutral masses $\to$ 24 physical quantities: $m_{a_0}$, $m_{K_0^\star}$, $m_{f_0^L}$, $m_{f_0^H}$, $m_\pi$, $m_K$, $m_\eta$, $m_{\eta'}$, $m_\rho$, $m_{K^\star}$, $m_\omega$, $m_\Phi$, $m_{a_1}$, $m_{K_1}$, $m_{f_1^H}$
- Charged and neutral decay widths $\to$ 21 physical quantities: $\Gamma_{\rho\to\pi\pi}$, $\Gamma_{\omega\to\pi\pi}$, $\Gamma_{K^\star\to K\pi}$, $\Gamma_{\Phi\to KK}$, $\Gamma_{a_1\to\rho\pi}$, $\Gamma_{a_1\to\pi\gamma}$, $\Gamma_{f_1\to K^\star K}$, $\Gamma_{K_0^\star\to K\pi}$, $\Gamma_{a_0\to KK}$, $\Gamma_{a_0\to\pi\eta}$, $\Gamma_{a_0\to\pi\eta'}$, $\Gamma_{f_0^{L/H}\to\pi\pi}$, $\Gamma_{f_0^{L/H}\to KK}$,

3

# Study of Self-similar Solution of Self-gravitating Non-relativistic Fluids

Balázs E. Szigeti [1, 2], Imre Ferenc Barna[2], Gergely Gábor Barnaföldi [2]

[1] Eötvös Loránd University

[2] Wigner Research Centre for Physics

# Motivation

- The properties and existence of the dark matter is one of the most fascinating question in cosmology.
- Our main goal of this research is to find **scaling solutions** of the gravitational fields, which can be good candidates to describe the evolution of the Universe or collapse of compact astrophysical objects
- We present a **dark fluid model** described as a non-relativistic and self-gravitating fluid
- We studied these coupled **non-linear differential equation** systems using self-similar time-dependent solutions

# The Model

We consider a set of coupled non-linear differential equations, which describes the **non-relativistic dynamics** of a compressible fluid with zero thermal conductivity and zero viscosity.

$$\partial_t \rho + \nabla(\rho \boldsymbol{u}) = 0$$
$$\partial_t \boldsymbol{u} + (\boldsymbol{u}\nabla)\boldsymbol{u} = -\frac{1}{\rho}\nabla p + \boldsymbol{g}$$
$$p = p(\rho)$$

Equation of State (Polytropic and Chaplygin gas)

$$p = -w\rho^n \qquad\qquad p = -\frac{A}{\rho^\alpha}$$

# Sedov-Taylor Ansatz

- We are reducing the PDE system into ODE system using Taylor *ansatz*:

$$u(r,t) = t^{-\alpha} f\left(\frac{r}{t^\beta}\right) \quad \rho(r,t) = t^{-\gamma} g\left(\frac{r}{t^\beta}\right)$$
$$\Phi(r,t) = t^{-\delta} h\left(\frac{r}{t^\beta}\right),$$

- $(f,g,h)$ **shape-functions** only depend on $\zeta = rt^{-\beta}$
- $\alpha, \beta, \gamma, \delta$ similarity exponents
- The $\beta$ describes **the rate of spread** of the spatial distribution
- Other exponents describe the **rate of decay** of the intensity of the corresponding field

# Result:

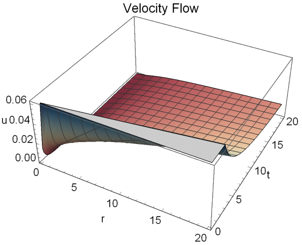
Velocity Flow
u
0.06
0.04
0.02
0.00
r
t

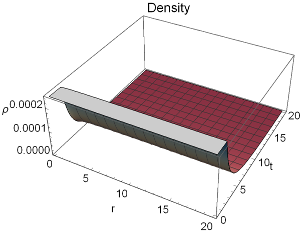
Density
ρ
0.0002
0.0001
0.0000
r
t

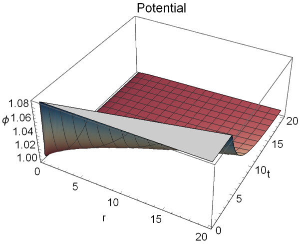
Potential
ϕ
1.08
1.06
1.04
1.02
1.00
r
t

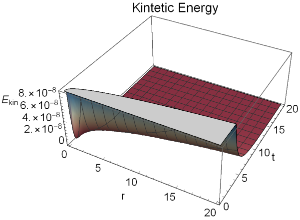
Kintetic Energy
$E_{kin}$
$8.\times 10^{-8}$
$6.\times 10^{-8}$
$4.\times 10^{-8}$
$2.\times 10^{-8}$
0
r
t

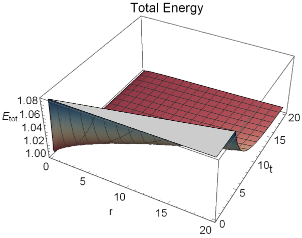
Total Energy
$E_{tot}$
1.08
1.06
1.04
1.02
1.00
r
t

# Propagation properties of spin degrees of freedom within the framework of relativistic hydrodynamics with spin

Victor E. Ambruș[1], Radosław Ryblewski[2], Rajeev Singh[2]

[1]Department of Physics, West University of Timișoara, Romania
[2]Institute of Nuclear Physics Polish Academy of Sciences, PL 31-342 Kraków, Poland

Zimányi School 2022

[V. E. Ambruș, R. Ryblewski and R. Singh, PRD **106** (2022) 014018]

# Spin tensor in the GLW pseudogauge

- $P^{\mu} = \int d\Sigma_{\nu} T^{\mu\nu}$ and $J^{\mu\nu} = \int d\Sigma_{\lambda} J^{\lambda,\mu\nu}$ are invariant under the **pseudogauge transformations**. F. W. Hehl, Rept. Math. Phys. **9** (1976) 55
- We use the **GLW** (Groot-van Leeuwen-van Weert) pseudogauge for the Dirac field.
- LTE for a polarized fluid can be described by

$$f^{\sigma}_{\rm eq} = \left[\exp\left(\beta p\cdot U - \sigma\xi - \frac{1}{2}\omega^{\mu\nu}s_{\mu\nu}\right) + 1\right], \quad s^{\mu\nu} = \frac{1}{m}\epsilon^{\mu\nu\alpha\beta}p_{\alpha}s_{\beta}, \tag{1}$$

where $\beta = T^{-1}$, $\xi = \mu/T$, $\sigma = \pm 1$ and $\omega^{\mu\nu}$ is the spin potential.
- The spin tensor comes out as:

$$S^{\lambda,\mu\nu} = (\mathcal{A}_1 + \mathcal{A}_3)U^{\lambda}\omega^{\mu\nu} + (2\mathcal{A}_1 - \mathcal{A}_3)U^{\lambda}U^{\alpha}U^{[\mu}\omega^{\nu]}{}_{\alpha} + \mathcal{A}_3(\Delta^{\lambda\alpha}U^{[\mu}\omega^{\nu]}{}_{\alpha} + U^{\lambda}\Delta^{\alpha[\mu}\omega^{\nu]}{}_{\alpha} + U^{\alpha}\Delta^{\lambda[\mu}\omega^{\nu]}{}_{\alpha}), \tag{2}$$

where

$$\mathcal{A}_1 = \frac{\mathfrak{s}^2}{9}\left[\left(\frac{\partial\mathcal{N}}{\partial\xi}\right)_{\beta} - \frac{2}{m^2}\left(\frac{\partial\mathcal{E}}{\partial\beta}\right)_{\xi}\right],$$

$$\mathcal{A}_3 = \frac{2\mathfrak{s}^2}{9}\left[\left(\frac{\partial\mathcal{N}}{\partial\xi}\right)_{\beta} + \frac{1}{m^2}\left(\frac{\partial\mathcal{E}}{\partial\beta}\right)_{\xi}\right]. \tag{3}$$

# Spin waves as transverse waves

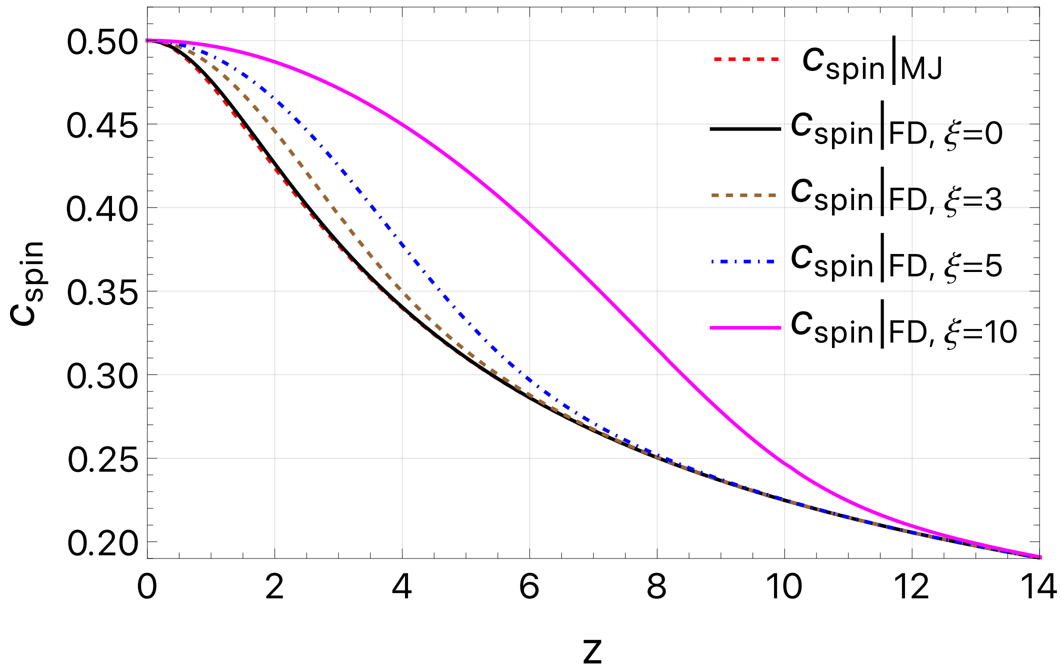


- Decomposing $\omega^{\mu\nu}$ into its electric $C_\kappa$ and magnetic $C_\omega$ components,

$$\omega^{\mu\nu} = \begin{pmatrix} 0 & C_{\kappa X} & C_{\kappa Y} & C_{\kappa Z} \\ -C_{\kappa X} & 0 & -C_{\omega Z} & C_{\omega Y} \\ -C_{\kappa Y} & C_{\omega Z} & 0 & -C_{\omega X} \\ -C_{\kappa Z} & -C_{\omega Y} & C_{\omega X} & 0 \end{pmatrix},$$

we find $\mathcal{C}_{\kappa Z} = \mathcal{C}_{\omega Z} = 0$, while

$$\left( \frac{\partial^2}{\partial t^2} - c_{\rm spin}^2 \frac{\partial^2}{\partial z^2} \right) \begin{pmatrix} \mathcal{C}_{\kappa X} \\ \mathcal{C}_{\kappa Y} \\ \mathcal{C}_{\omega X} \\ \mathcal{C}_{\omega Y} \end{pmatrix} = 0, \quad c_{\rm spin}^2 = -\frac{1}{4}\frac{\mathcal{A}_3}{\mathcal{A}_1} \to \begin{cases} \frac{1}{2}, & \frac{m}{T} \to 0, \\ \sqrt{\frac{T}{2m}}, & \frac{m}{T} \to \infty. \end{cases} \quad (4)$$